Ph.D Thesis

Potential aspects supporting δ-aminolevulinic acid-induced photodynamic therapy

TRAN TIEN TAI

Kyoto Institute of Technology

2014

Contents

Abbreviation 1
General introduction 2
Chapter 1. Neurotransmitter transporter family including SLC6A6 and SLC6A13 contributes to the 5-aminolevulinic acid (ALA)-induced accumulation of protoporphyrin IX and photo-damage, through uptake of ALA by cancerous cells
Introduction 19
Material and methods 20
Results 23
Discussion 26
References 28
Chapter 2. p53 directly regulates the transcription of the human frataxin gene and the unregulation in tumor cells decreases the utilization of mitochondrial iron
Introduction 44
Material and methods 45
Results 46
Discussion 48
References 50
Conclusion 60
List of publications 61
Acknowledgement 62

Abbreviations

ALA	δ-aminolevulinic acid
ALAS	δ-aminolevulinic acid synthase
FECH	Ferrochelatase
FRDA	Friedreich's ataxia
GABA	γ-aminobutyric acid
NTT	Neurotransmitter transpoter
P53RE	p53 responsive element
PDR	Photodynamic reaction
PDT	Photodynamic therapy
PPIX	Protoporphyrin IX
PS	Photosensitizer
SLC	Solute carrier

General introduction

1. Photodynamic therapy (PDT)

1.1 Introduction

PDT was accidently discovered over 100 years ago by medical student Oscar Raab when he was studying the interaction of fluorescent dyes on infusaria (1). Although patients were being successfully treated by this process for a wide variety of cancers, particularly of the skin by the early 1900's, the reaction of this therapy was rediscovered by Lipson and Schwartz nearly 50 years later (2, 3). However until the 1970's, working with porphyrin compounds, Dougherty created a complete solution including commercially suitable photosensitizing drug, reliable light sources and appropriate clinical trials proving the value of PDT to the oncologic community, which was in contrast to previous iterations (4). This marked the age of PDT initializing. And from then on, Dougherty has been considered as the "The Father of PDT".

Briefly, photodynamic therapy (PDT) is an elegant light based oncologic intervention. A photosensitizer (PS) is applied then activated by light of the appropriate wavelength and intensity (Fig. 1). This creates the photodynamic reaction (PDR) selectively eliminating the tumor tissue, which will be clarified in following parts.

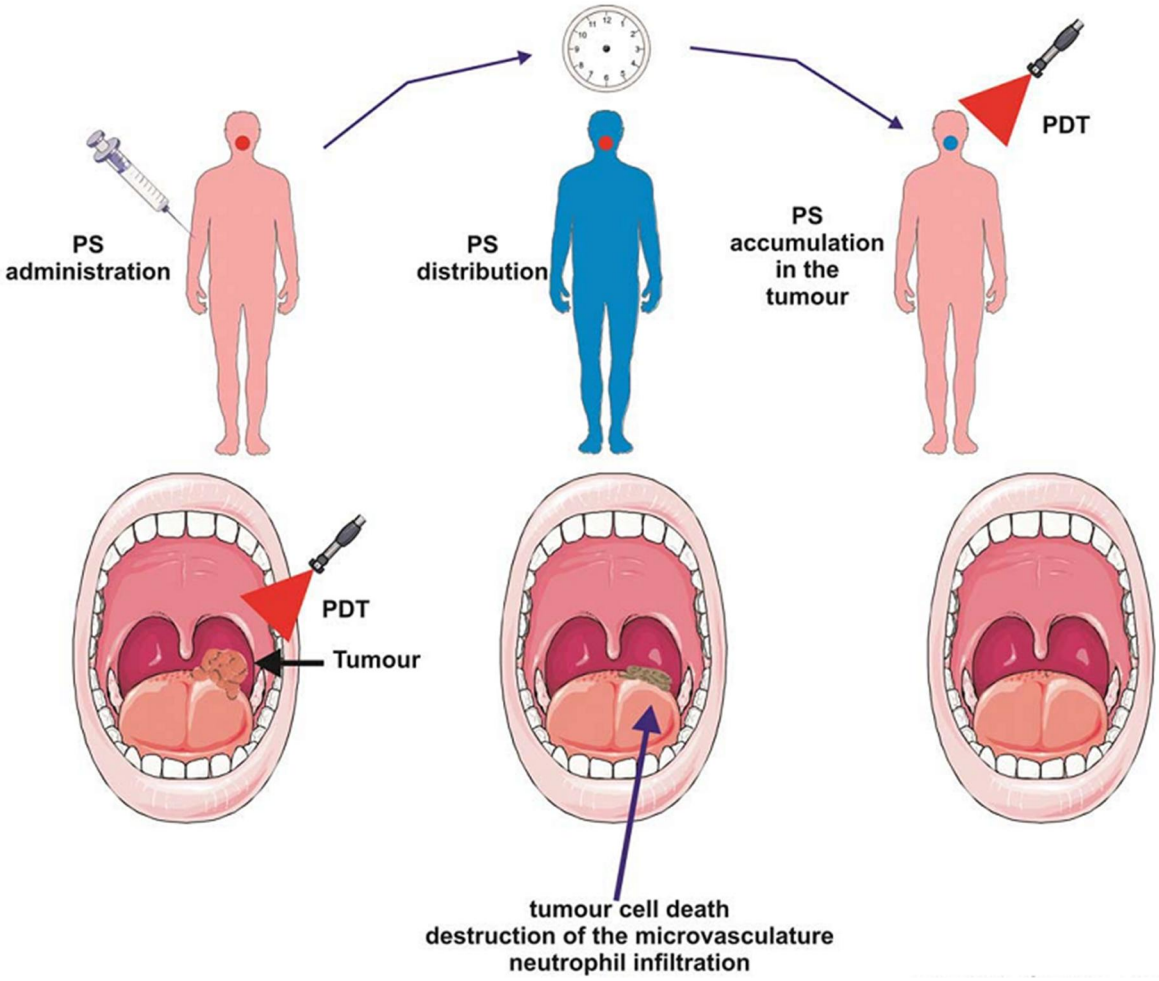

Figure 1. General procedures of PDT

1.1 PDT mechanism

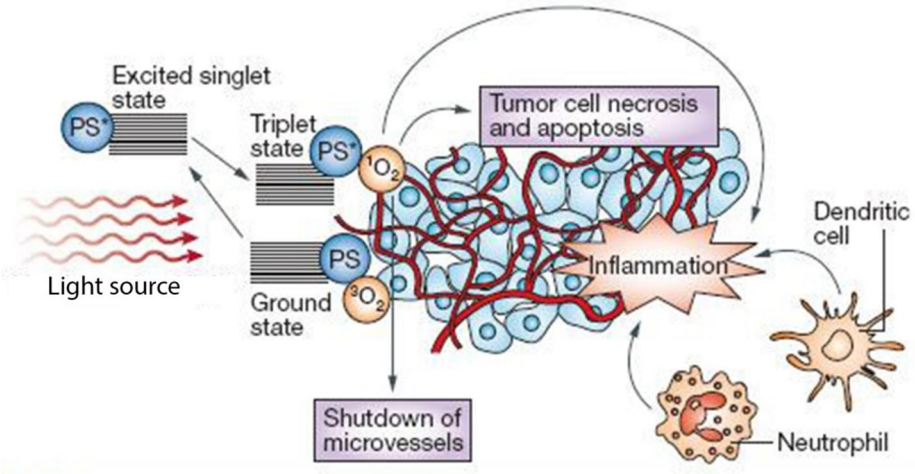

Figure 2. General mechanism of PDT

PDT consists of 3 essential components (Fig. 2): (1) PS, a light-absorbing compound that initiates a photochemical or photophysical reaction, (2) light and (3) oxygen (5, 6). None of these is individually toxic, but after two stages of PDT procedures, administration of a light-sensitive PS and irradiation with a light of appropriate wavelength, together they initiate a photochemical reaction that culminates in the generation of a highly reactive product termed singlet oxygen ($^1O_2$), an excited or energized form of molecular oxygen characterized by the opposite spin of a pair of electrons that is less stable and more reactive than the normal triplet oxygen (O_2).

Singlet oxygen has a radius of destruction measured in nanometers yet this allows for a significant and complex cascade of events resulting in local, regional, and systemic alteration of both tumor and immune response so that reliable tumor control is possible. Tumor destruction from PDT can occur by both apoptotic (programmed) pathways and necrosis (non-programmed) pathways (7, 8).

Generally, when high light intensity is employed, the tumor cells are rapidly ablated by necrosis (9). The cellular and subcellular membrane destruction is rapid. Most probably, calcium (10) and metabolic byproducts (11) are released which are not compatible with cell function and repair functions are overwhelmed, leading to ablation of the tumor cell. This also leads o release of cytokines and toxic chemicals from, for example, the mitochondria (12). This leakage will then create lethal damage in cells nearby (13) (bystander effect) as well as creating a regional and systematic reaction.

In contrast, apoptotic death may be initiated by PDT, generally when low light doses are employed (14). During apoptosis, the cells cease to function and undergo an orderly and programmed dissolution. No bystander effect or immune response is expected as no toxic chemicals are leaked. Apoptotic pathways are found in both tumor and normal cells across many species including bacteria. It appears that apoptosis is a well conserved method of the organism to eliminate damaged cells. PDT appears to be able to activate this pathway.

In similarity to tumor cells, endothelial cells of the vascular systems can concentrate PS (15-17). The neovasculature of malignancy is also felt to be leaky due to poor and incomplete cellular borders and may serve as an additional means for PS accumulation in tumor regions as it leaks through. In contrast, the surrounding normal vasculature in the non-tumorous region may facilitate PS clearance.

1.2 Photosensitizers

PS agents are natural or synthetic structures that transfer light energy (18). While thousands upon thousands of structures have been identified as PS agents, perhaps two dozen have been well characterized and only about one dozen employed in clinical trials. Of these perhaps two or three are Food and Drug Administration (or equivalent) approved and commercially available. In the clinic, a successful PS agent has most of the following characteristics: nontoxic till activated, hydrophilic for easy systemic application, activated by a clinically useful light wavelength, and reliable generation of the PDR. It also concentrates in tumor, clears normal tissue, is eliminated from the patient relatively rapidly, is a nontoxic degradation product with ease of synthesis, pain free therapy and, just as importantly, commercial availability.

1.3 PDT application

Many patients have already been treated with PDT for a variety of neoplasms with excellent results. With the use of fibre-optic systems, light can be targeted accurately into many parts of the body for the treatment of tumours. Therefore, many studies showing the results of clinical trials emphasise the importance of PDT for the treatment of endoscopically accessible tumours. In addition, selectivity of PDT is achieved from the preferential localisation of the PS in the target tissue and from the fact that only the irradiated areas will be affected as the PS is per se non-toxic.

Photosensitiser	**Chemical class**	**Indications**	**Date of approval and country**
Haematoporphyrin derivative (HPD)	Porphyrin	Barrett's oesophagus	1994 in Canada. Now in more han 125 countries (EU, Canada, Japan, China, India and Russia, among others)
Porfimer sodium		Cervical dysplasia Cervical cancer Lung cancer Superficial gastric cancer Oesophageal adenocarcinoma Superficial bladder cancer	
Tetra(m-hydoxyphenyl) chlorin mTHPC, Temoporfin	Chlorin	Palliative head and neck cancer	2001 in EU

ALA	Porphyrin	Actinic keratoses	2000 in USA
ALA-methyl ester	Porphyrin	Actinic keratoses Basal cell carcinoma	2001 in EU

Table 1. Clinically applied PSs

Table 1 shows the PSs approved for clinical use and their applications for cancer and premalignant diseases. HPD has been approved for the treatment of early stage and advanced lung cancers, superficial gastric cancer, oesophageal adenocarcinoma, cervical cancer and bladder cancer. The chlorine derivative mTHPC, has also been approved in the European Union (EU) for the palliative treatment of head and neck cancer. Apart from HPD, mTHPC and Temoporfin, no other systemically administered PSs are currently used for the treatment of neoplasms (19). However, topically applied PSs (ALA and ALA-methylester) have been approved for the treatment of both tumor and other proliferative skin diseases (basal cell carcinomas and actinic keratosis) (20).

The use of PDT for disseminated tumors and precancerous lesions is under investigation for carcinomatosis, pituitary tumors and glioblastoma, but represents now an effective adjuvant treatment. Although in these cases PDT alone is not effective to achieve the complete remission of neoplastic diseases, at least this treatment can be useful in prolonging survival and/or improving the life quality of patients.

In addition, the growing interest in new PSs and their use for cancer therapy have extended PDT applications to other medical fields, especially in ophthalmology and dermatology. The benzoporphyrin derivative monoacid ring A (BPD-MA) or verteporfin has been approved for the treatment of neovascular age-related macular degeneration and other ocular diseases (5, 21). ALA and ALA-methylester are currently being used for treatment of acne and psoriasis in dermatology, and also for diagnostic purposes in proliferating diseases. In this sense, after topical or systemic ALA application, PPIX is induced in epithelial tumors, and can then be visualized under exposure to appropriated light (blue light), thus improving the possibilities of tumor detection by fluorescence in comparison to white light endoscopy. The applications of this approach are not only for superficial skin neoplasms but also for others of internal location (e.g., urinary tract tumours). ALA hexylester has improved the detection rates of both flat and papillary lesions in the imaging of bladder tumors, and it has recently been approved for this use in 26 European countries (19, 22).

2. Heme biosysthesis pathway (Fig. 3)

2.1 Introduction

The synthesis of ALA is the first and rate-limiting step in the biosynthesis of heme (23-25). ALA is normally synthesized in mitochondria in the condensation reaction between glycine and succinyl-CoA (Fig. 3). The reaction is catalyzed by ALA synthase (ALAS) and requires pyridoxal-5-phosphate (PLP) as a cofactor. In mammals, two isoforms of ALA synthase have been identified: ALAS1, which is a housekeeping enzyme and ALAS2, which is expressed only in erythroid precursors (26).

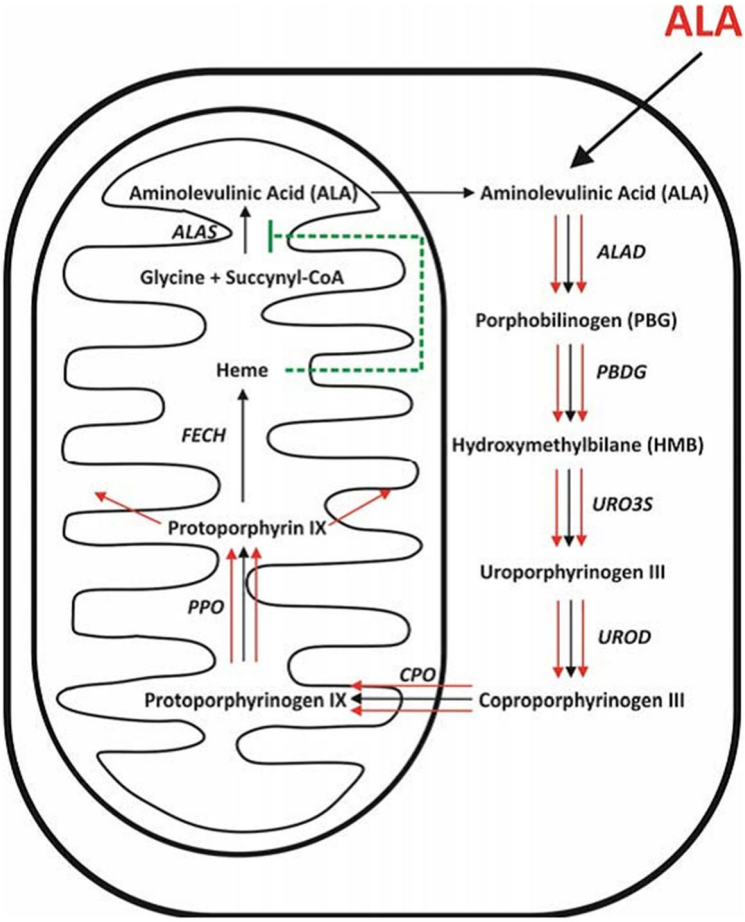

Figure 3. Heme biosynthesis pathway

After being synthesized, ALA reaches cytosol, where it undergoes a condensation reaction. The reaction occurs between two ALA molecules with the aid of zinc-dependent enzyme – aminolevulinate dehydratase (ALAD) – and leads to the formation of porphobilinogen (PBG). ALAD, also known as porphobilinogen synthase (PBGS) comprises four homodimers, each of them having one active site (27). Two molecules of ALA bind non-symmetrically to the active site, finally leading to the synthesis of PBG (28). The next step in heme biosynthesis involves combining four molecules of PBG to form an unstable tetrapyrolle - hydroxymethylbilane (HMB). The reaction is catalyzed by porphobilinogen deaminase (PBDG), an enzyme containing dipyrromethane in its active site. Dipyrromethane is a co-factor covalently bound to the enzyme and consists of two PBG molecules. Four additional molecules of PBG attach to dipyrromethane leading to the formation of hexapyrolle. Afterwards, in the hydrolytic reaction, cleavage of the distal tetrapyrolle occurs, resulting in the release of HMB (29). Hydroxymethylbilane can then enter two pathways. The first one uses uroporphyrinogen III synthase (URO3S) to close the HMB macrocycle leading to conversion of tetrapyrolle to uroporphyrinogen III. Alternatively, HMB can undergo spontaneous cyclization, which leads to the formation of uroporphyrinogen I (30). Uroporphyrinogen decarboxylase (UROD) catalyzes decarboxylation of all four acetate side chain of uroporphyrinogen III to methyl groups (31).

The product of preceding reaction – coproporphyrinogen II is transported to the intermembrane space of mitochondria probably by peripheral-type benzodiazepine receptors (PBR) (32, 33). Coproporphyrinogen oxidase (CPO) then catalyzes the conversion to coporoporphyrinogen III to protoporporphyrinogen IX with the release of H_2O_2 and CO_2. The reaction provides vinyl groups by oxidative decarboxylation of propionate groups on pyrolle rings A and B (34). There are two forms of CPO: oxygen-dependent found in aerobic organisms, and oxygen-independent, in anaerobic and facultative bacteria (35). In mammals, oxygen-dependent CPO is originally synthesized in cytosol with unusually long N-terminal sequence targeting it to the mitochondria (36). Finally, CPO is situated in the mitochondrial intermembrane space with a fraction loosely bound to the inner membrane (37). The next intermediate in heme biosynthesis, PPIX, is synthesized in the mitochondria and requires FAD-containing protoporphyrinogen oxidase (PPO) (38, 39). PPO catalyzes conversion of protoporphyrinogen IX to PPIX in the six-electron oxidation. The reaction requires oxygen as a terminal electron acceptor and leads to removal of six hydrogens from protoporphyrinogen IX (40). Ferrochelatase (FECH), another rate-limiting enzyme, is responsible for insertion of Fe^{2+} into PPIX. The reaction occurs on the inner surface of the inner mitochondrial membrane (41). This stage leads to the formation of the final product, heme, and completes the heme biosynthetic pathway.

2.2 δ-aminolevulinic acid

ALA is a prodrug that is enzymatically converted to PPIX, a potent PS. ALA can be topically placed, orally introduced or intravenously injected. Whilst the treatment is uncomfortable when topically placed, no systemic phototoxicity occurs. Regarding to the nature of ALA, it is a naturally occurring compound, the early intermediate in the heme biosynthesis pathway. For therapeutic purposes ALA is administered topically or systemically and penetrates non-selectively into all cells, where it is metabolized to an active sensitizer PPIX. The bio-activation of ALA utilizes the enzyme machinery of the heme biosynthesis pathway. Although nearly all human cell types express the enzymes involved in the heme synthesis, a distinct activity of the enzymes in tumor as compared with normal cells leads to a higher PPIX accumulation within transformed cells (40).

2.2.1 Effect of exogenous ALA administration

PPIX is a strong photosensitizer, which assembles in mitochondria of tumor cells leading to their damage after light exposure. Although all enzymes involved in the heme biosynthetic pathway are necessary, only two of them: ALAS1 and FECH are considered to be rate-limiting. Normally, the activity of ALAS, is regulated by heme through the negative feedback mechanism. Heme binds to the heme-regulatory motif in mitochondrial targeting sequence of ALAS and therefore prevents transport of ALAS1 precursor to mitochondria (42). Moreover, there is evidence that heme not only regulates ALAS1 mitochondrial import but also attenuates its transcription (43, 44). Normally, the feedback mechanism leads to the production of PPIX in such amounts that can be efficiently converted to heme by FECH. Exogenous administration of ALA bypasses the natural regulation that heme exerts on

ALA synthesis, which leads to increased production of PPIX (40). The efficacy of FECH is then too low to convert excessively produced PPIX to heme, which results in the accumulation of PPIX within cells. About 4-6 hours after administration of ALA, when PPIX is already synthesized, target cells are exposed to light, which leads to excitation of the photosensitizer and formation of $^1O_2$ that exerts cytotoxic effects.

2.2.2 Selectivity of PPIX accumulation in tumor cells in response to ALA administration

PPIX has been found to preferentially accumulate in tumor as compared with normal cells. This phenomenon can be explained by differences in heme biosynthetic pathway between non-malignant and malignant cells. It has been shown that decreased activity of FECH (45-48) and limited availability of iron (49) in tumor cells contribute to increased PPIX accumulation. Enhanced activity of enzymes leading to production of PPIX, such as ALAD, UROD (50), or PBGD (45, 50, 51) has also been observed in tumor cells.

2.2.3 ALA transporters

Several reports have appeared describing that multiple uptake systems are involved in the transport of ALA, and may differ among different types of tumor cell (52). Dipeptide transporters PEPT1 (SLC15A1) and PEPT2 (SLC15A2) may mediate ALA uptake in tumor. PEPT1 is expressed only in the small intestine, and was found to be increased in colon cancer cells, while PEPT2 is ubiquitously expressed, but its expression was found not to be elevated in neoplastic cells (53, 54). Furthermore, H^+-coupled amino acid transporter PAT1 (SLC36A1) can transport ALA across the brush border membrane of intestinal cells.

2.2.4 Potential ALA transporters

- Amino acid transport systems in the plasma membrane of mammalian cells

Functional studies based on saturability of transport, substrate specificity, kinetic behavior, mode of energization, and mechanisms of regulation performed in perfused organs, isolated cells, and purified plasma membranes led to the identification of a mutiplicity of transport agencies in the plasma membrane of mammalian cells (55-58). From these studies it is evident that a particular transport system carries different amino acids and that amino acid transport systems show overlapping specificities. Different cells contain a distinct set of transport systems in their plasma membranes, as a combination of common or almost ubiquitous (e.g., systems A, ASC, L, y^+ and X_{AG}) and tissue-specific transport systems (e.g., systems $B^{o,+}$, N^m, and $b^{o,+}$ as well as variants of common transport systems). It has been proposed that this arrangement permits both fine regulation of substrate and cell-specific amino acid flows and economy in the number of structures mediating cellular and interorgan amino acid fluxes (58, 59).

- Glutamine transporters

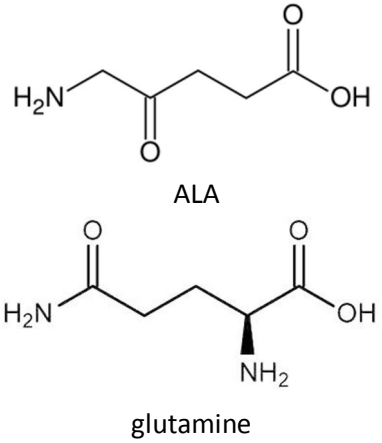

Figure 4. Homologous structure of ALA and

The amino acid glutamine has been the focus of many studies in physiology and medicine due to its important pleiotropic roles in metabolism and tissue homeostasis. As discussed in detail in many articles, glutamine serves as an essential metabolic precursor in nucleotide, glucose and amino sugar biosynthesis, glutathione homeostasis and protein synthesis (60). Moreover, the growth of proliferating cells such as fibroblasts, lymphocytes and enterocytes relies heavily on glutamine as an oxidative energy source. Although classified as "nonessential" in most biochemistry text books, glutamine appears essential for the viability and growth of cells maintained in tissue culture, as first demonstrated by the seminal work of Harry Eagle in the 1950s (61). The nitrogen-rich character and unique metabolism of this amino acid allow it to serve as the major interorgan ammonia shuttle. Glutamine also supports tissue homeostasis by participation in intercellular substrate cycles in the brain and liver and in fetal-placental nutrient exchange. Indeed, the fact that glutamine is the most abundant amino acid in the plasma (at 600–800 μmol) and exhibits extremely rapid cellular turnover rates (62) is a testament to its diverse utility in mammalian physiology. It is the expression of specific transporters in the plasma membrane, however, that affords the prodigious intercellular exchange and metabolism of glutamine.

Some cancer cell lines also display addiction to glutamine despite the fact that glutamine is a nonessential amino acid that can be synthesized from glucose. The high rate of glutamine uptake exhibited by glutamine-dependent cells does not appear to result solely from its role as a nitrogen donor in nucleotide and amino acid biosynthesis. Instead, glutamine plays a required role in the uptake of essential amino acid and in maintaining activation of TOR kinase. Moreover, in many cancer cells, glutamine is the primary mitochondrial substrate and is required to maintain mitochondrial membrane potential and integrity as well as support of the NADPH production needed for redox control and macromolecular synthesis (63). Aside from relation to cancer cells, the substrates glutamine and ALA share the carbon skeleton structure, as well.

- γ-aminobutyric acid (GABA) transporters

The SLC6 family is among the largest SLC families, containing 20 genes that encode a group of highly similar transporter proteins. These proteins perform transport of amino acids and amino acid derivatives into cells, using co-transport of extracellular Na^+ as a driving force for substrate translocation against chemical gradients (4, 63, 64). The SLC6 transporters are secondary active transporters (4), because they use the electrochemical potential difference across the cell membrane of Na^+ as energy source for transport. In addition, the SLC6 transporters are further classified as

symporters, in that the coupled transport of Na^+ is performed in the same direction as substrate transport, although a few members also exhibit antiport activity by performing counter-transport of K^+ (65). The majority of the SLC6 transporters has a well-defined biological function and physiological role, including known endogenous substrates, and is divided into four subclasses on the basis of sequence similarity and substrate specificity (64). All the SLC6 neurotransmitter transporters (NTTs) are expressed in the central nervous system, where their primary physiological role is regulation of neurotransmitter homeostasis. However, some of them are also found in other tissues, where they serve important physiological functions. Because the NTTs genes were among the founding gene members of the SLC6 gene family, alternate designations for the family are often used, such as the "neurotransmitter-sodium symporters," the "sodium-neurotransmitter symporter family," or the "Na^+/Cl^- neurotransmitter transporter" family (66, 67). A series of breakthroughs in the understanding of the structure and function of bacterial transporters related to the SLC6 family have rejuvenated the SLC6 NTTs research field in a manner not seen since the cloning of the first transporter genes in the early 1990s (60-62, 68-70). These advances have promoted a profound increase in the understanding of the structural biology and molecular pharmacology of the SLC6 NTTs, in addition to highlighting the importance of understanding other aspects of transporter biology, including cellular mechanisms for transporter regulation by post-translational modifications, protein-protein interactions, and trafficking.

2.3 Iron utilization for heme biosythesis

2.3.1 Frataxin

Frataxin, a conserved protein found ubiquitously in prokaryotes and eukaryotes, is required for the cellular regulation of iron homeostasis. Although of extreme interest to many chemists and biologists alike, frataxin's exact role in helping cells regulate iron chemistry and metal availability remains controversial at best. Frataxin has been proposed to participate in at least five different capacities: 1) as an iron chaperone during cellular heme and iron-sulfur (Fe-S) cluster production, 2) as an iron-storage protein during conditions of iron overload, 3) as an aid in the repair of oxidatively damaged aconitase Fe-S clusters, 4) as a factor that controls cellular oxidative stress by moderating the concentration of reactive oxygen species (ROS), 5) as an active participant in pathways involving energy conversion and oxidative phosphorylation.

It has also been reported that frataxin also interacts with FECH (71). As iron is present in large excess in Dyfh1 cells, it was described that yeast cells lacking frataxin are deficient in iron use by FECH. Thus, it was suggested that frataxin could deliver Fe^{2+} to complete Fe-S clusters and heme biosynthesis (71-74). While frataxin has been postulated to be responsible for maintaining iron in a bioavailable or soluble form, it cannot be excluded that this protein might play a role as an Fe donor for this metal to be incorporated into a molecule of protoporphyrin. The hypothesis that frataxin may also act as a Fe chaperone for heme synthesis becomes more significant from these data. Moreover, the precise function of frataxin in heme metabolism and hemoprotein biogenesis is not yet clarified. In

addtion, a combination of X-ray absorption spectroscopy and nuclear magnetic resonance studies was used to confirm that monomeric frataxin binds high spin ferrous iron in a six-coordinate metal–ligand coordination environment utilizing in part carboxylate oxygens as ligands from conserved acidic residues in frataxin's helix-1. Additional nuclear magnetic resonance studies confirm frataxin's FECH docking surface is constructed predominantly by helical surface residues on the protein's helical face. Complex formation in this manner would allow for metal delivery between the two protein partners, providing the ferrous iron required for in vivo heme biosynthesis (75).

2.3.2 Friedreich's ataxia

Friedreich's ataxia (FRDA) is the most common autosomal recessive ataxia, in the vast majority of patients, due to homozygous expansion of a guanine–adenine–adenine (GAA) trinucleotide repeat in intron 1 of the frataxin gene on chromosome 9q13 (76). The majority (>95%) of patients with FRDA are homozygous for large expansions of a GAA triplet–repeat sequence (66–1800 triplets) located within the first intron of the gene X25, which encodes the protein frataxin (76). Therefore, the mutation causes a defect of transcription (77), and lack of frataxin, a small mitochondrial protein, is the accepted cause of the entire complex clinical and pathological phenotype of FRDA. The disease affects central and peripheral nervous systems: heart, skeleton, and endocrine pancreas. Concretely, FRDA is characterized clinically by progressive gait and limb ataxia; signs of upper motoneuron dysfunction including dysarthria, areflexia, and loss of the senses of position and vibration; cardiomyopathy; diabetes mellitus; and secondary skeletal abnormalities.

Frataxin is required for the in vivo production of Fe-S clusters and is believed to play a direct role in their assembly. An Fe-S cluster deficiency was identified in FRDA patients early in the recognition of the disorder, suggesting the need for frataxin in Fe-S cluster assembly (78). This idea was supported by knockout mice showing similar disease phenotypes (79) and more recently in the bacterial system (80). The majority of the direct frataxin in vivo Fe-S cluster correlations come again however from studies in the yeast system (81-83). Suppressing Yfh1 expression results in respiratory deficiency, mitochondrial iron accumulation and reduced Fe-S enzyme activity while non Fe-S containing enzymes remained active (81). Additional studies suggest that frataxin may not be essential for Fe-S cluster assembly, but it does improve the efficiency of the assembly process (82). A direct interaction between frataxin and the assembly apparatus proteins has been detected (83-85), and the requirement of frataxin for the maturation of Fe-S clusters in yeast has been confirmed (86). Taken together, these data suggest frataxin plays a direct role in the cellular assembly of Fe-S clusters.

2.3.3 The tumor suppressor protein p53

The critical tumor suppressor p53 plays important roles in cell-cycle arrest, apoptosis, senescence, or differentiation in response to various genotoxic and cellular stresses, including oxidative stress (87-89). As a guardian of the genome, the inactivation of wild-type p53 function by direct gene mutation or disruption of pathways important for p53 activation is a prerequisite for the development of most human cancers (90-92). The p53 protein can be divided into three regions: 1) the amino terminus,

containing the transcriptional activation region; 2) the central portion of the molecule, containing highly conserved sequence blocks throughout which the majority of oncogenic mutations are located; and 3) the carboxyl terminus, containing both oligomerization and nuclear localization sequences.

The tumor suppressor protein p53 is an important transcriptional factor for multiple proteins involved in the cellular damage response, and an intact p53 response prevents mutations from accumulating by increasing the expression of genes that inhibit cell growth (93). p53 is mutated or lost in numerous cancer cells, which is closely related to altered expression of pro-oxidant and antioxidant proteins (94). A link between frataxin and p53 was observed in Caenorhabditis elegans where the absence of cep-1, a homologue of p53, significantly suppressed the increase in lifespan induced by reduced expression of the frataxin homologue frh-1 (95, 96). It was showed that colon carcinoma MIP101, DLD2 and HT29 cells were found to lack endogenous expression of frataxin (97) whereas non transformed cells highly expressed frataxin (98). This provides evidence for a close link between the activity of p53 and the expression of frataxin to maintain normal functions of cells. Recently, by examination of frataxin level with knockdown or mutation of p53, it has been found that the transcription of the frataxin gene was directly p53-dependent (99). In detail, the reporter activity of the promoter in the mouse frataxin gene increased, accompanied by p53RE elements located at -307 to -298 and -294 to -285 bp of the promoter. The expression of frataxin was found to be stimulated in cancerous MethA cells expressing mutated p53 by expression of the wild-type p53. The ChIP assay of the mouse frataxin promoter revealed that p53 was associated with p53RE in NIH3T3 cells, but not in the case of MethA cells. Based on the data obtained that the expression of frataxin in cells expressing wild-type p53 was higher than that in human tumor cells with mutated p53, and p53 silencing decreased the expression of frataxin in HEK293T cells, p53 directly regulates the expression of frataxin.

2.3.4 p53-frataxin and ALA-PDT

Targeted disruption of frataxin gene in mouse liver caused decreased life span and tumor formation, which is likely to be a typical feature of patients with FRDA who exhibit various types of cancer and reduced life span (100). It was also found that knockdown of frataxin led to an increase in the ALA-induced photo-damage with the accumulation of protoporphyrin (101). Lately, it was reported that stable overexpression of frataxin in tumor cells decreased the accumulation of ALA-induced protoporphyrin and photo-damage (99). In addition, direct evidence that frataxin functions as an iron chaperon and can prompt the maturation of FECH by forming the Fe-S cluster of the enzyme was also provided (99). In turn, the dysfunction of p53 in cancerous cells leads to the decrease of frataxin expression and the general function of mitochondria including FECH, thereby enhancing ALA-PDT.

References

1. Allison, R. R., H. C. Mota and C. H. Sibata (2004) Clinical PD/PDT in North America: An historical review. *Photodiagnosis and photodynamic therapy* **1**, 263-77.
2. Lipson, R. L. and E. J. Baldes (1960) Photosensitivity and heat. *Arch Dermatol* **82**, 517-20.
3. Lipson, R. L. and E. J. Baldes (1960) The photodynamic properties of a particular hematoporphyrin derivative. *Arch Dermatol* **82**, 508-16.
4. Dougherty, T. J. (1984) Photodynamic therapy (PDT) of malignant tumors. *Crit Rev Oncol Hematol* **2**, 83-116.
5. Dolmans, D. E., D. Fukumura and R. K. Jain (2003) Photodynamic therapy for cancer. *Nat Rev Cancer* **3**, 380-7.
6. Dougherty, T. J., C. J. Gomer, B. W. Henderson, G. Jori, D. Kessel, M. Korbelik, J. Moan and Q. Peng (1998) Photodynamic therapy. *J Natl Cancer Inst* **90**, 889-905.
7. Igney, F. H. and P. H. Krammer (2002) Death and anti-death: tumour resistance to apoptosis. *Nat Rev Cancer* **2**, 277-88.
8. Oleinick, N. L., R. L. Morris and I. Belichenko (2002) The role of apoptosis in response to photodynamic therapy: what, where, why, and how. *Photochemical & Photobiological Sciences* **1**, 1-21.
9. Oleinick, N. L. and H. H. Evans (1998) The photobiology of photodynamic therapy: cellular targets and mechanisms. *Radiat Res* **150**, S146-56.
10. Ding, X., Q. Xu, F. Liu, P. Zhou, Y. Gu, J. Zeng, J. An, W. Dai and X. Li (2004) Hematoporphyrin monomethyl ether photodynamic damage on HeLa cells by means of reactive oxygen species production and cytosolic free calcium concentration elevation. *Cancer Lett* **216**, 43-54.
11. Henderson, B. W. and J. M. Donovan (1989) Release of prostaglandin E2 from cells by photodynamic treatment in vitro. *Cancer Res* **49**, 6896-900.
12. Henderson, B. W., B. Owczarczak, J. Sweeney and T. Gessner (1992) Effects of photodynamic treatment of platelets or endothelial cells in vitro on platelet aggregation. *Photochem Photobiol* **56**, 513-21.
13. Dahle, J., O. Kaalhus, J. Moan and H. B. Steen (1997) Cooperative effects of photodynamic treatment of cells in microcolonies. *Proc Natl Acad Sci U S A* **94**, 1773-8.
14. Agarwal, M. L., M. E. Clay, E. J. Harvey, H. H. Evans, A. R. Antunez and N. L. Oleinick (1991) Photodynamic therapy induces rapid cell death by apoptosis in L5178Y mouse lymphoma cells. *Cancer Res* **51**, 5993-6.
15. Castano, A. P., T. N. Demidova and M. R. Hamblin (2005) Mechanisms in photodynamic therapy: Part three—Photosensitizer pharmacokinetics, biodistribution, tumor localization and modes of tumor destruction. *Photodiagnosis and photodynamic therapy* **2**, 91-106.
16. Castano, A. P., T. N. Demidova and M. R. Hamblin (2005) Mechanisms in photodynamic therapy: part two—cellular signaling, cell metabolism and modes of cell death. *Photodiagnosis and photodynamic therapy* **2**, 1-23.
17. Abels, C. (2004) Targeting of the vascular system of solid tumours by photodynamic therapy (PDT). *Photochem Photobiol Sci* **3**, 765-71.
18. Allison, R. R., G. H. Downie, R. Cuenca, X.-H. Hu, C. J. H. Childs and C. H. Sibata (2004) Photosensitizers in clinical PDT. *Photodiagnosis and photodynamic therapy* **1**, 27-42.
19. Juzeniene, A., Q. Peng and J. Moan (2007) Milestones in the development of photodynamic therapy and fluorescence diagnosis. *Photochem Photobiol Sci* **6**, 1234-45.
20. Babilas, P., M. Landthaler and R. M. Szeimies (2006) Photodynamic therapy in dermatology. *Eur J Dermatol* **16**, 340-8.
21. Brown, S. B. and K. J. Mellish (2001) Verteporfin: a milestone in opthalmology and photodynamic therapy. *Expert Opin Pharmacother* **2**, 351-61.
22. Schmidbauer, J., F. Witjes, N. Schmeller, R. Donat, M. Susani, M. Marberger and P. C. B. S. G. Hexvix (2004) Improved detection of urothelial carcinoma in situ with hexaminolevulinate fluorescence cystoscopy. *J Urol* **171**, 135-8.
23. Ajioka, R. S., J. D. Phillips and J. P. Kushner (2006) Biosynthesis of heme in mammals. *Biochim Biophys Acta* **1763**, 723-36.
24. Fukuda, H., A. Casas and A. Batlle (2005) Aminolevulinic acid: from its unique biological function to its star role in photodynamic therapy. *Int J Biochem Cell Biol* **37**, 272-6.
25. Ishizuka, M., F. Abe, Y. Sano, K. Takahashi, K. Inoue, M. Nakajima, T. Kohda, N. Komatsu, S. Ogura and T. Tanaka (2011) Novel development of 5-aminolevurinic acid (ALA) in cancer diagnoses and therapy. *Int Immunopharmacol* **11**, 358-65.
26. Riddle, R. D., M. Yamamoto and J. D. Engel (1989) Expression of delta-aminolevulinate synthase in avian cells: separate genes encode erythroid-specific and nonspecific isozymes. *Proc Natl Acad Sci U S A* **86**, 792-6.

27. Anderson, P. M. and R. J. Desnick (1979) Purification and properties of delta-aminolevulinate dehydrase from human erythrocytes. *J Biol Chem* **254**, 6924-30.
28. Jarret, C., F. Stauffer, M. E. Henz, M. Marty, R. M. Luond, J. Bobalova, P. Schurmann and R. Neier (2000) Inhibition of Escherichia coli porphobilinogen synthase using analogs of postulated intermediates. *Chem Biol* **7**, 185-96.
29. Shoolingin-Jordan, P. M., A. Al-Dbass, L. A. McNeill, M. Sarwar and D. Butler (2003) Human porphobilinogen deaminase mutations in the investigation of the mechanism of dipyrromethane cofactor assembly and tetrapyrrole formation. *Biochem Soc Trans* **31**, 731-5.
30. Jordan, P. M. and J. S. Seehra (1979) The biosynthesis of uroporphyrinogen III: order of assembly of the four porphobilinogen molecules in the formation of the tetrapyrrole ring. *FEBS Lett* **104**, 364-6.
31. Straka, J. G. and J. P. Kushner (1983) Purification and characterization of bovine hepatic uroporphyrinogen decarboxylase. *Biochemistry* **22**, 4664-72.
32. Taketani, S., H. Kohno, T. Furukawa and R. Tokunaga (1995) Involvement of peripheral-type benzodiazepine receptors in the intracellular transport of heme and porphyrins. *J Biochem* **117**, 875-80.
33. Taketani, S., H. Kohno, M. Okuda, T. Furukawa and R. Tokunaga (1994) Induction of peripheral-type benzodiazepine receptors during differentiation of mouse erythroleukemia cells. A possible involvement of these receptors in heme biosynthesis. *J Biol Chem* **269**, 7527-31.
34. Yoshinaga, T. and S. Sano (1980) Coproporphyrinogen oxidase. II. Reaction mechanism and role of tyrosine residues on the activity. *J Biol Chem* **255**, 4727-31.
35. Dailey, H. A. (2002) Terminal steps of haem biosynthesis. *Biochem Soc Trans* **30**, 590-5.
36. Delfau-Larue, M. H., P. Martasek and B. Grandchamp (1994) Coproporphyrinogen oxidase: gene organization and description of a mutation leading to exon 6 skipping. *Hum Mol Genet* **3**, 1325-30.
37. Grandchamp, B., N. Phung and Y. Nordmann (1978) The mitochondrial localization of coproporphyrinogen III oxidase. *Biochem J* **176**, 97-102.
38. Dailey, T. A. and H. A. Dailey (1998) Identification of an FAD superfamily containing protoporphyrinogen oxidases, monoamine oxidases, and phytoene desaturase. Expression and characterization of phytoene desaturase of Myxococcus xanthus. *J Biol Chem* **273**, 13658-62.
39. Koch, M., C. Breithaupt, R. Kiefersauer, J. Freigang, R. Huber and A. Messerschmidt (2004) Crystal structure of protoporphyrinogen IX oxidase: a key enzyme in haem and chlorophyll biosynthesis. *EMBO J* **23**, 1720-8.
40. Collaud, S., A. Juzeniene, J. Moan and N. Lange (2004) On the selectivity of 5-aminolevulinic acid-induced protoporphyrin IX formation. *Curr Med Chem Anticancer Agents* **4**, 301-16.
41. Wu, C. K., H. A. Dailey, J. P. Rose, A. Burden, V. M. Sellers and B. C. Wang (2001) The 2.0 A structure of human ferrochelatase, the terminal enzyme of heme biosynthesis. *Nat Struct Biol* **8**, 156-60.
42. Munakata, H., J. Y. Sun, K. Yoshida, T. Nakatani, E. Honda, S. Hayakawa, K. Furuyama and N. Hayashi (2004) Role of the heme regulatory motif in the heme-mediated inhibition of mitochondrial import of 5-aminolevulinate synthase. *J Biochem* **136**, 233-8.
43. Srivastava, G., I. A. Borthwick, D. J. Maguire, C. J. Elferink, M. J. Bawden, J. F. Mercer and B. K. May (1988) Regulation of 5-aminolevulinate synthase mRNA in different rat tissues. *J Biol Chem* **263**, 5202-9.
44. Surinya, K. H., T. C. Cox and B. K. May (1997) Transcriptional regulation of the human erythroid 5-aminolevulinate synthase gene. Identification of promoter elements and role of regulatory proteins. *J Biol Chem* **272**, 26585-94.
45. Hinnen, P., F. W. de Rooij, M. L. van Velthuysen, A. Edixhoven, R. van Hillegersberg, H. W. Tilanus, J. H. Wilson and P. D. Siersema (1998) Biochemical basis of 5-aminolaevulinic acid-induced protoporphyrin IX accumulation: a study in patients with (pre)malignant lesions of the oesophagus. *Br J Cancer* **78**, 679-82.
46. Krieg, R. C., S. Fickweiler, O. S. Wolfbeis and R. Knuechel (2000) Cell-type specific protoporphyrin IX metabolism in human bladder cancer in vitro. *Photochem Photobiol* **72**, 226-33.
47. Hefti, M., F. Holenstein, I. Albert, H. Looser and V. Luginbuehl (2011) Susceptibility to 5-aminolevulinic acid based photodynamic therapy in WHO I meningioma cells corresponds to ferrochelatase activity. *Photochem Photobiol* **87**, 235-41.
48. Ohgari, Y., Y. Nakayasu, S. Kitajima, M. Sawamoto, H. Mori, O. Shimokawa, H. Matsui and S. Taketani (2005) Mechanisms involved in delta-aminolevulinic acid (ALA)-induced photosensitivity of tumor cells: relation of ferrochelatase and uptake of ALA to the accumulation of protoporphyrin. *Biochem Pharmacol* **71**, 42-9.
49. Stout, D. L. and F. F. Becker (1990) Heme synthesis in normal mouse liver and mouse liver tumors. *Cancer Res* **50**, 2337-40.
50. Navone, N. M., C. F. Polo, A. L. Frisardi, N. E. Andrade and a. M. del C. Baille (1990) Heme biosynthesis in human breast cancer—mimetic "in vitro" studies and some heme enzymic activity levels. *International Journal of Biochemistry* **22**, 1407-11.

51. Kondo, M., N. Hirota, T. Takaoka and M. Kajiwara (1993) Heme-biosynthetic enzyme activities and porphyrin accumulation in normal liver and hepatoma cell lines of rat. *Cell Biol Toxicol* **9**, 95-105.
52. Rodriguez, L., A. Batlle, G. Di Venosa, S. Battah, P. Dobbin, A. J. Macrobert and A. Casas (2006) Mechanisms of 5-aminolevulinic acid ester uptake in mammalian cells. *Br J Pharmacol* **147**, 825-33.
53. Rodriguez, L., A. Batlle, G. Di Venosa, A. J. MacRobert, S. Battah, H. Daniel and A. Casas (2006) Study of the mechanisms of uptake of 5-aminolevulinic acid derivatives by PEPT1 and PEPT2 transporters as a tool to improve photodynamic therapy of tumours. *Int J Biochem Cell Biol* **38**, 1530-9.
54. Anderson, C. M., M. Jevons, M. Thangaraju, N. Edwards, N. J. Conlon, S. Woods, V. Ganapathy and D. T. Thwaites (2010) Transport of the photodynamic therapy agent 5-aminolevulinic acid by distinct H+-coupled nutrient carriers coexpressed in the small intestine. *J Pharmacol Exp Ther* **332**, 220-8.
55. Bannai, S., H. N. Christensen, J. V. Vadgama, J. C. Ellory, E. Englesberg, G. G. Guidotti, G. C. Gazzola, M. S. Kilberg, A. Lajtha, B. Sacktor and et al. (1984) Amino acid transport systems. *Nature* **311**, 308.
56. Christensen, H. N. (1985) On the strategy of kinetic discrimination of amino acid transport systems. *J Membr Biol* **84**, 97-103.
57. Christensen, H. N. (1989) Distinguishing amino acid transport systems of a given cell or tissue. *Methods Enzymol* **173**, 576-616.
58. Christensen, H. N. (1990) Role of amino acid transport and countertransport in nutrition and metabolism. *Physiol Rev* **70**, 43-77.
59. Christensen, H. N. (1993) Amino acid nutrition: a two-step absorptive process. *Nutr Rev* **51**, 95-100.
60. Neu, J., V. Shenoy and R. Chakrabarti (1996) Glutamine nutrition and metabolism: where do we go from here ? *FASEB J* **10**, 829-37.
61. Eagle, H. (1955) Nutrition needs of mammalian cells in tissue culture. *Science* **122**, 501-14.
62. Darmaun, D., D. E. Matthews and D. M. Bier (1986) Glutamine and glutamate kinetics in humans. *Am J Physiol* **251**, E117-26.
63. Wise, D. R. and C. B. Thompson (2010) Glutamine addiction: a new therapeutic target in cancer. *Trends Biochem Sci* **35**, 427-33.
64. Christensen, H. N., M. Liang and E. G. Archer (1967) A distinct Na+-requiring transport system for alanine, serine, cysteine, and similar amino acids. *J Biol Chem* **242**, 5237-46.
65. Utsunomiya-Tate, N., H. Endou and Y. Kanai (1996) Cloning and functional characterization of a system ASC-like Na+-dependent neutral amino acid transporter. *J Biol Chem* **271**, 14883-90.
66. Arriza, J. L., M. P. Kavanaugh, W. A. Fairman, Y. N. Wu, G. H. Murdoch, R. A. North and S. G. Amara (1993) Cloning and expression of a human neutral amino acid transporter with structural similarity to the glutamate transporter gene family. *J Biol Chem* **268**, 15329-32.
67. Shafqat, S., B. K. Tamarappoo, M. S. Kilberg, R. S. Puranam, J. O. McNamara, A. Guadano-Ferraz and R. T. Fremeau, Jr. (1993) Cloning and expression of a novel Na(+)-dependent neutral amino acid transporter structurally related to mammalian Na+/glutamate cotransporters. *J Biol Chem* **268**, 15351-5.
68. Kanai, Y. (1997) Family of neutral and acidic amino acid transporters: molecular biology, physiology and medical implications. *Curr Opin Cell Biol* **9**, 565-72.
69. Sato, H., M. Tamba, T. Ishii and S. Bannai (1999) Cloning and expression of a plasma membrane cystine/glutamate exchange transporter composed of two distinct proteins. *J Biol Chem* **274**, 11455-8.
70. Wang, H., M. Tamba, M. Kimata, K. Sakamoto, S. Bannai and H. Sato (2003) Expression of the activity of cystine/glutamate exchange transporter, system x(c)(-), by xCT and rBAT. *Biochem Biophys Res Commun* **305**, 611-8.
71. Lesuisse, E., R. Santos, B. F. Matzanke, S. A. Knight, J. M. Camadro and A. Dancis (2003) Iron use for haeme synthesis is under control of the yeast frataxin homologue (Yfh1). *Hum Mol Genet* **12**, 879-89.
72. Cavadini, P., H. A. O'Neill, O. Benada and G. Isaya (2002) Assembly and iron-binding properties of human frataxin, the protein deficient in Friedreich ataxia. *Hum Mol Genet* **11**, 217-27.
73. Adinolfi, S., M. Trifuoggi, A. S. Politou, S. Martin and A. Pastore (2002) A structural approach to understanding the iron-binding properties of phylogenetically different frataxins. *Hum Mol Genet* **11**, 1865-77.
74. Yoon, T. and J. A. Cowan (2004) Frataxin-mediated iron delivery to ferrochelatase in the final step of heme biosynthesis. *J Biol Chem* **279**, 25943-6.
75. Bencze, K. Z., T. Yoon, C. Millan-Pacheco, P. B. Bradley, N. Pastor, J. A. Cowan and T. L. Stemmler (2007) Human frataxin: iron and ferrochelatase binding surface. *Chem Commun (Camb)*, 1798-800.
76. Campuzano, V., L. Montermini, M. D. Molto, L. Pianese, M. Cossee, F. Cavalcanti, E. Monros, F. Rodius, F. Duclos, A. Monticelli, F. Zara, J. Canizares, H. Koutnikova, S. I. Bidichandani, C. Gellera, A. Brice, P. Trouillas, G. De Michele, A. Filla, R. De Frutos, F. Palau, P. I. Patel, S. Di Donato, J. L. Mandel, S. Cocozza, M. Koenig and M. Pandolfo (1996) Friedreich's ataxia: autosomal recessive disease caused by an intronic GAA triplet repeat expansion. *Science* **271**, 1423-7.

77. Grabczyk, E. and K. Usdin (2000) The GAA*TTC triplet repeat expanded in Friedreich's ataxia impedes transcription elongation by T7 RNA polymerase in a length and supercoil dependent manner. *Nucleic Acids Res* **28**, 2815-22.
78. Rotig, A., P. de Lonlay, D. Chretien, F. Foury, M. Koenig, D. Sidi, A. Munnich and P. Rustin (1997) Aconitase and mitochondrial iron-sulphur protein deficiency in Friedreich ataxia. *Nat Genet* **17**, 215-7.
79. Puccio, H., D. Simon, M. Cossee, P. Criqui-Filipe, F. Tiziano, J. Melki, C. Hindelang, R. Matyas, P. Rustin and M. Koenig (2001) Mouse models for Friedreich ataxia exhibit cardiomyopathy, sensory nerve defect and Fe-S enzyme deficiency followed by intramitochondrial iron deposits. *Nat Genet* **27**, 181-6.
80. Vivas, E., E. Skovran and D. M. Downs (2006) Salmonella enterica strains lacking the frataxin homolog CyaY show defects in Fe-S cluster metabolism in vivo. *J Bacteriol* **188**, 1175-9.
81. Chen, O. S., S. Hemenway and J. Kaplan (2002) Inhibition of Fe-S cluster biosynthesis decreases mitochondrial iron export: evidence that Yfh1p affects Fe-S cluster synthesis. *Proc Natl Acad Sci U S A* **99**, 12321-6.
82. Duby, G., F. Foury, A. Ramazzotti, J. Herrmann and T. Lutz (2002) A non-essential function for yeast frataxin in iron-sulfur cluster assembly. *Hum Mol Genet* **11**, 2635-43.
83. Muhlenhoff, U., J. Gerber, N. Richhardt and R. Lill (2003) Components involved in assembly and dislocation of iron-sulfur clusters on the scaffold protein Isu1p. *EMBO J* **22**, 4815-25.
84. Gerber, J., U. Muhlenhoff and R. Lill (2003) An interaction between frataxin and Isu1/Nfs1 that is crucial for Fe/S cluster synthesis on Isu1. *EMBO Rep* **4**, 906-11. Epub 2003/08/30.
85. Ramazzotti, A., V. Vanmansart and F. Foury (2004) Mitochondrial functional interactions between frataxin and Isu1p, the iron-sulfur cluster scaffold protein, in Saccharomyces cerevisiae. *FEBS Lett* **557**, 215-20.
86. Stehling, O., H. P. Elsasser, B. Bruckel, U. Muhlenhoff and R. Lill (2004) Iron-sulfur protein maturation in human cells: evidence for a function of frataxin. *Hum Mol Genet* **13**, 3007-15.
87. Zhu, D., J. Wu, C. Spee, S. J. Ryan and D. R. Hinton (2009) BMP4 mediates oxidative stress-induced retinal pigment epithelial cell senescence and is overexpressed in age-related macular degeneration. *J Biol Chem* **284**, 9529-39.
88. Sandor, J., T. Ambrus and I. Ember (1995) [The function of the p53 gene suppressor in carcinogenesis]. *Orv Hetil* **136**, 1875-83. A p53 gen szuppresszor funkciojanak szerepe a karcinogenezisben.
89. Mansur, C. P. (1997) The regulation and function of the p53 tumor suppressor. *Adv Dermatol* **13**, 121-66.
90. Walker, D. R., J. P. Bond, R. E. Tarone, C. C. Harris, W. Makalowski, M. S. Boguski and M. S. Greenblatt (1999) Evolutionary conservation and somatic mutation hotspot maps of p53: correlation with p53 protein structural and functional features. *Oncogene* **18**, 211-8.
91. Pavletich, N. P., K. A. Chambers and C. O. Pabo (1993) The DNA-binding domain of p53 contains the four conserved regions and the major mutation hot spots. *Genes Dev* **7**, 2556-64.
92. Freeman, J., S. Schmidt, E. Scharer and R. Iggo (1994) Mutation of conserved domain II alters the sequence specificity of DNA binding by the p53 protein. *EMBO J* **13**, 5393-400.
93. Liu, D. and Y. Xu (2011) p53, oxidative stress, and aging. *Antioxid Redox Signal* **15**, 1669-78.
94. Asher, G., J. Lotem, B. Cohen, L. Sachs and Y. Shaul (2001) Regulation of p53 stability and p53-dependent apoptosis by NADH quinone oxidoreductase 1. *Proc Natl Acad Sci U S A* **98**, 1188-93.
95. Ventura, N., S. L. Rea, A. Schiavi, A. Torgovnick, R. Testi and T. E. Johnson (2009) p53/CEP-1 increases or decreases lifespan, depending on level of mitochondrial bioenergetic stress. *Aging Cell* **8**, 380-93.
96. Torgovnick, A., A. Schiavi, R. Testi and N. Ventura (2010) A role for p53 in mitochondrial stress response control of longevity in C. elegans. *Exp Gerontol* **45**, 550-7.
97. Schulz, T. J., R. Thierbach, A. Voigt, G. Drewes, B. Mietzner, P. Steinberg, A. F. Pfeiffer and M. Ristow (2006) Induction of oxidative metabolism by mitochondrial frataxin inhibits cancer growth: Otto Warburg revisited. *J Biol Chem* **281**, 977-81.
98. Ristow, M., M. F. Pfister, A. J. Yee, M. Schubert, L. Michael, C. Y. Zhang, K. Ueki, M. D. Michael, 2nd, B. B. Lowell and C. R. Kahn (2000) Frataxin activates mitochondrial energy conversion and oxidative phosphorylation. *Proc Natl Acad Sci U S A* **97**, 12239-43.
99. Sawamoto, M., T. Imai, M. Umeda, K. Fukuda, T. Kataoka and S. Taketani (2013) The p53-dependent expression of frataxin controls 5-aminolevulinic acid-induced accumulation of protoporphyrin IX and photo-damage in cancerous cells. *Photochem Photobiol* **89**, 163-72.
100. Thierbach, R., T. J. Schulz, F. Isken, A. Voigt, B. Mietzner, G. Drewes, J. C. von Kleist-Retzow, R. J. Wiesner, M. A. Magnuson, H. Puccio, A. F. Pfeiffer, P. Steinberg and M. Ristow (2005) Targeted disruption of hepatic frataxin expression causes impaired mitochondrial function, decreased life span and tumor growth in mice. *Hum Mol Genet* **14**, 3857-64.
101. Ohgari, Y., Y. Miyata, T. Miyagi, S. Gotoh, T. Ohta, T. Kataoka, K. Furuyama and S. Taketani (2011) Roles of porphyrin and iron metabolisms in the delta-aminolevulinic acid (ALA)-induced accumulation of protoporphyrin and photodamage of tumor cells. *Photochem Photobiol* **87**, 1138-45.

Chapter 1

Neurotransmitter transporter family including SLC6A6 and SLC6A13 contributes to the 5-aminolevulinic acid (ALA)-induced accumulation of protoporphyrin IX and photo-damage, through uptake of ALA by cancerous cells

Introduction

Becoming commercial application from 1970s (1), PDT is still getting perfection with accumulative updating studies. Initially, PS protoporphyrin has been used as an effective one (1). From the other PSs latter found and applied, ALA differentiated to be a potential prodrug of PDT due to its natural conversion to PPIX, which follows the heme biosynthesis pathway. The application of ALA-induced accumulation of protoporphyrin has been used for the diagnosis of bladder cancer, endometriosis lesions of cervix and lung cancer, and the subsequent PDT has advantages over systemic administration in that the entire body does not face sensitization. ALA-induced PDT has produced good clinical outcomes in various medical fields including brain and breast cancer (2, 3). Regarding the mechanism of the therapy, exogenous ALA is effectively converted to protoporphyrin and creates the accumulation of this PS with a specific manner in cancerous cells (4-6). This specificity comes from various mechanisms. Concretely, the accumulation of protoporphyin is contributed by limited capacity of FECH (7, 8), the enzyme consists of an iron-sulfur cluster, catalyzes insert of ion into protoheme and decreases its activity due to reduced expression of mitochondrial iron-chaperon frataxin unregulated by p53 (9). Thus, the mitochondrial dysfunctions including decreased utilization of iron in this organelle and recycling of heme-iron via heme degradation possibly play crucial role in ALA-PDT. Several addition factor including porphyrin-biosynthetic enzymes and protoporphyrin-exporter pump proteins are also involved in the accumulation of protoporphyrin (7, 10, 11). The efficiency of this ALA-based therapy is achieved by the preferential uptake of this protoporphyrin precursor in cancerous cells, as well.

Despite of the extensive application of therapy, that selective penetration of ALA is still not elucidated well. Thus far, there is not such a specific transporter for ALA. Though, it has been reported to share transporters with several compounds (12-14). Among of them, glutamine/glutamate and GABA transporters were suggested to be potential candidates. These lead us to clarify the relationship between glutamine/glutamate and GABA transporters family ALA-PDT.

From the investigation, some of potential glutamine and glutamate transporters have been chosen and then experimented. ASCT2 comes from the ASC system, originally named for three of its preferred substrates (alanine, serine, cysteine) (15). The first mammalian glutamine transporter gene was isolated in 1996 from a mouse testis cDNA, encoding for a 553 amino acid protein with functional of System ASC (16). It was termed ASCT2 to distinguish it from ASCT1, a System ASC isoform isolated in 1993 that does not transport glutamine (17, 18). In addition, ASCT2 transporter are part of the excitatory amino acid transporter family composed thus far ASCT1 and several glutamate transporter (19). SNAT3 belongs to former system A and N transport families share common sequential and functional characteristics; therefore, they have been reclassified as a single family, SLC38A or System N/A Transport (SNAT) family. The members of the SNAT transporter

system family mostly convey L-glutamine, L-histidine, L-asparagine, and L-alanine across cell membranes (20, 21). SNAT3 (also referred to as SN1 or NAT or SLC38A3) expression in the brain is largely confined to astrocytes. Abundant expression of the SNAT3 protein is detected in astrocytes throughout the brain and retina, but SNAT3 is absent from neurons and oligodendrocytes (22, 23). SNAT3 mRNA is also abundant in liver, kidney, heart, skeletal muscle, and adipose tissue (24-26), but the protein is not detected in heart or skeletal muscle (22). SNAT3 bears the hallmarks of System N, in terms of its Na^+ dependence and preference for glutamine and histidine. And xCT, cystine/glutamate antiporter, is a protein that in humans is encoded by the *SLC7A11* gene (27, 28). SLC7A11 is a member of a heteromeric Na^+-independent anionic amino acid transport system highly specific for cystine and glutamate. In this system, designated system Xc(-), the anionic form of cystine is transported in exchange for glutamate. SLC7A11 has also been termed 'xCT'.

Mentioning on GABA, in previous pharmacological studies, ALA uptake was found inhibited by GABA and some amino acid relating to this family of transporters with the Na^+ and Cl^- dependent manner in several cell lines (29). These observations suggested that Na^+- and Cl^--dependent neurotransmitter transporters (or BETA transporters) may take up ALA into cells. These transporters are comprised of SLC6A6, SLC6A8, SLC6A11, SLC6A12, and SLC6A13, which are involved in the transport of GABA-related molecules are mainly expressed in neural cells. Though, these were also found to be expressed in several tumor cells (30). These lead us to clarify the relationship between glutamine/glutamate and GABA transporters family ALA-PDT. We started with examining whether these compounds inhibited the protoporphyrin accumulation in tumor cells. And here we found that the expression of neurotransmitter transporters SLC6A6 and SLC6A13 increased the ALA uptake, resulting in the ALA-induced accumulation of protoporphyrin and photo-damage. The tissue distribution of these transporters and the cancerous expression were also found.

We started with examining whether these compounds inhibited the protoporphyrin accumulation in tumor cells. And here we found that the expression of neurotransmitter transporters SLC6A6 and SLC6A13 increased the ALA uptake, resulting in the ALA-induced accumulation of protoporphyrin and photo-damage. The tissue distribution of these transporters and the cancerous expression were also found.

Materials and Methods

Materials

An INST blot membrane of human cell line lysates was a product of IMGENEX (San Diego, CA). Restriction endonucleases and DNA modifying enzymes were from Takara Co. (Tokyo, Japan) and Toyobo Co. (Tokyo, Japan). Antibodies for SLC6A6 and myc-tag were products of MBL Co. Ltd. (Tokyo, Japan). Polyclonal antibodies for actin (sc-1615) and SLC6A13 (bs-13259R) were obtained

from Santa Cruz Biotechnology (Santa Cruz, CA), and from Bioss Co. (Boston, MA), respectively. ALA, ALA-methylester and SLC6A6 esiRNA (EMU054651) were purchased from Sigma Co. (St. Louis, MI). SLC6A13 siRNA (sc-41960) was a product of Santa Cruz. All other chemicals were of analytical grade.

Construction of SLC6A6, SLC6A8, SLC6A12 and SLC6A13 expression plasmids

The cDNAs for human for ASCT2, SNAT3 and xCT were obtained from from a human kidney cDNA library (Takara Ltd., Tokyo, Japan) and ligated into the *Eco*RI site of pCDNA3.1-c-myc (Invitrogen, Carlsbad, CA). Primers used were 5'-GCTGGATATCTGCAGAATTCATGGTGGCCG and 5'-AGTCCAGTGGGTGGAATTCCATGACTGAT for ASCT2, 5'-GGATATCTGCAGAATTCATGGAGGCGCCTTTGCAGA and 5'CCAGTGTGGTGGAATTCAGGCGACAGCCCTACCCT for SNAT3, 5'-GCTGGATATCTGCAGAATTCATGGTCAGAA and 5'-AGTCCAGTGTGGTGGAATTCTAACTTATCT for xCT.

In similarity, SLC6A6, SLC6A8, SLC6A12 and SLC6A13 cDNAs were created with primers 5'-AAGAATTCATGGCCACCAAGGAGAA and 5'-AAGAATTCCACATCATGGTCTCCACA for SLC6A6; 5'-AAGAATTCATGGCGAAGAAGAGCGCC and 5'-AAGAATTCCCACATGACACTCTCCAC for SLC6A8; 5'-AAGAATTCATGGACGGGAAGGTGGC and 5'-AAGAATTCGTACAAATGGGTCTCCTT for SLC6A12; and 5'-AAGAATTCATGGATAGCAGGGTCTCA and 5'-AAGGAATTCGTAGCAGTCAGACTCTAG for SLC6A13.

All the nucleotide sequences of these cDNAs were confirmed by DNA sequencing.

Cell cultures

Human epithelial cervical cancer HeLa cells, and human embryonic kidney HEK293T were grown in Dulbecco's modified Eagle's medium (DMEM) supplemented with 7% fetal calf serum (FCS), penicillin (100 units/ml) and streptomycin (100 μg/ml). Human colon cancer DLD-1 cells were grown in RPMI 1640 medium containing 7% fetal calf serum (FCS) and antibiotics. HEK293T cells were transfected with pcDNA3-SLC6A6, pcDNA3-SLC6A8, pcDNA3-SLC6A12 and pcDNA3-SLC6A13 using HilyMax (Dojin Co. Ltd., Tokyo) and incubated for 16 h, while DLD-1 and HeLa cells transfected with siRNAs using Lipofectamine RNAiMAX (Invitrogen) were cultured for 48 h.

Protoporphyrin accumulation

Cultured cells were incubated with ALA (500 μM) for 4 h (5, 9). Protoporphyrin was extracted from the cells with 96% ethanol containing 0.5 M HCl (5, 7, 9). The amount of protoporphyrin was determined by fluorescence spectrophotometry, as previously described (7). With glutamine/glutamate-present experiments, we washed cells twice with DMEM supplemented with 7%

FCS, penicillin (100 units/ml) and streptomycin (100 μg/ml) but not glutamine and phenol red before carrying out incubations.

Uptake of ALA by the cells

The cells (5 x 10^5) were incubated in FCS-free DMEM in the presence of 20 μM ALA for a specific period, and the medium was then withdrawn. ALA in medium was derivatized primarily by acetylacetone with heat treatment. In detail, ALA-pyrole produced by the condensation of ALA with 1M sodium acetate pH 4.6 was extracted by acetylacetone. Finally, the absorbance of solution, with cherry-red color created by reacting of formed ALA derivative described and Erhlich's reagent (31), was measured by spectrophotometry at the wavelength 555nm.

Exposure of the cells to light

The cells were incubated with ALA (100-500 μM) for 6 h, and 1.0 ml of fresh drug-free medium was then added. Irradiation with visible light was carried out under sterile conditions, using a fluorescence lamp, in a CO_2 incubator, as described previously (5, 7). Briefly, the light was filtered through a glass plate (thickness: 0.5 cm) to omit UV light and given from the bottom of the culture plate to achieve a uniform delivery to the entire plate. The distance of culture plates from light source was 8.0 cm. The increase of the temperature was maintained to be less than 2ºC by using a thermo-couple device during exposure to light. The irradiation was carried out with white light of fluorescence lamp for 10 minutes with dose 0.81J/cm^2 and intensity 35 mW/cm^2. Then, after 20-minute incubation, cells were pulsed with 3-(4,5-dimethylthiazol-2-yl)-2,5-diphenyltetrazolium bromide (MTT, 500 μg/ml) for 2 h and resultant MTT formazan was solubilized with isopropanol. Absorbance at 590 nm was measured with a Microplate Reader NJ2001 (Japan InterMed. Co., Tokyo, Japan). Each experiment was carried out in triplicate or quadruplicate. Cell viability (cell survival) is expressed as a percentage of cells without light exposure.

Thus far, irradiation in PDT includes coherent lasers, non-coherent lamps and advanced light-emitting diodes. Though, the wide range 400-700 nm used in the present study had been applied in previous studies on tumor cell lines (32, 33). Also in a later publication, spectrum handled was from 420-800 nm (34). However, recent irradiation is often excluded the infrared range to prevent hyperthermia. Then, not aiming to such particular treatment, we used low-cost source, white light from a fluorescence lamp with filtered UV range and hyperthermia controlled by thermal-couple device.

Immunoblotting

The lysates from human cultured cells were subjected to sodium dodecylsulfate-polyacrylamide gel electrophoresis (SDS-PAGE) and electroblotted onto poly(vinylidene difluoride) (PVDF) membrane (Bio-Rad Laboratories, Hercules, CA). Immunoblotting was carried out with antibodies for SLC6A6, SLC6A13, myc-tag and actin, as the primary antibodies (5, 9).

Immunohistochemistry

The surgically resected specimens of colon cancer were embedded in paraffin. The paraffine sections were routinely deparaffinized and rehydrated. For deparaffinization, the sections were incubated in xylene for 5 min each of 4 times. For rehydration, the sections were incubated in 100% ethanol for 5 min, 95% ethanol for 5 min, 70% ethanol for 5 min, 50% ethanol for 5 min, distilled H_2O for 5 min and then 10 mM Tris-HCl (pH 7.5) containing 150 mM NaCl for 5 min, sequentially. Then, they were stained with hematoxylin & eosin. Otherwise, immunohistochemical staining was carried out. The thin sections were subjected to heat-induced epitope retrieval in High Target Retrieval solution (Dako, Glostrup, Denmark), and then incubated with primary antibodies for SLC6A6 or SLC6A13 for 56 min. The immunohistochemical staining was performed using BenchMark XT (Ventana Medical Systems, Inc., Tucson, AZ, USA), a fully automated IHC/ISH staining instrument.

Statistics

Results are shown as mean ± S.D., and were analyzed using unpaired Student's t-test. All statistical analyses were considered significant at the level of $p<0.05$ using Microsoft Excel® 2010 version 14.0.4756.1000 (© 2010 Microsoft Corporation) (9, 35).

Results

The decrease of ALA-induced formation of protoporphyrin by glutamine

We (7) previously showed that the ALA uptake in cancerous cells was greater than that in non-tumor cells. Due to the similar C5-amino-acid structure of ALA and its origin from glutamate in plants (36, 37), ALA may interact with the glutamine/glutamate uptake system. To evaluate the effect of these homologues on the transport of ALA, we first examined whether glutamine and glutamate affect the ALA-induced accumulation of protoporphyrin using HeLa cells. Initially, measurement of protoporphyrin IX accumulation resulted in effective inhibition in the presence of glutamine but not glutamate (Fig. 1A). To further examine the inhibitive manner of glutamine, a concentration array of this amino acid was assessed. However, in this experiment, glutamine did not affect the formation of protoporphyrin (Fig. 1B). Besides, we also attempted to examine the role of glutamate transporter by 3-hydroxy-DL-aspartate (HAsp), an inhibitor of glutamate transporter (38). The data did not show any effect of glutamate on the accumulation (Fig. 1C).

Expression of ASCT2, xCT and SNAT3 enhanced ALA-induced accumulation of protoporphyrin

Despite the unstable inhibition of glutamine, we tried examining the effect of some glutamine transporters on accumulation of photosensitizer. Examination showed that ASCT2 and SNAT3 negligibly contributed to the elevation of protoporphyrin as compared with the control (Fig. 2A,B) whereas xCT did not (data not shown). Expression of respective DNAs was examined by Westernblot,

as well. However, there was only existence of SNAT3 detected by anti-Myc antibody (Fig. 2C). Due to the fluctuating inhibition of glutamine and insignificant effect of its transporter, we stopped the assessment of relation of this amino acid to ALA-PDT.

The decrease of ALA-induced formation of protoporphyrin by neurotransmitters GABA, taurine, β-alanine

Since the structure of ALA is an analogous to that of neurotransmitter GABA (14), ALA may interact with the GABA uptake system, as well. Similar procedures with glutamine and glutamate were carried out with GABA-related compouds, which were supposed to be inhibitors of ALA uptake, using colon cancer DLD-1 cells. Such homologues we used were β-alanine, creatine and taurine. The fluorescence pattern with ethanol extracts of the cells treated with 500 μM ALA for 4 h showed a maximum peak at 637 nm with excitation at 400 nm, which was consistent with that of standard protoporphyrin. When incubation of cells with ALA plus GABA was carried out, the accumulation decreased, in a dose-dependent manner (Fig. 3A). The treatment with taurine or β-alanine was also inhibitory to the protoporphyrin formation. Creatine did not decrease the accumulation of protoporphyrin. In the absence of ALA, no accumulation of protoporphyrin in cells with GABA or other compounds was observed (data not shown). The effect of GABA-related compounds on the ALA-induced formation of protoporphyrin was also examined with HeLa cells. The addition of GABA, β-alanine, creatine or taurine decreased the accumulation of protoporphyrin by incubation of HeLa cells with ALA, but the decrease was less than that obtained with DLD-1 cells (Fig. 3B). These results suggested that glutamine and GABA-related transporters could transport ALA through the plasma membrane.

Expression of SLC6A6, SLC6A8 and SLC6A13 enhanced ALA-induced accumulation of protoporphyrin and photo-damage in HEK263T cells

Since the uptake of ALA and GABA-related compounds through the plasma membrane shared the same transporters, the relationship of the structure of GABA transporter to ALA transporter was examined. A homology search of the human protein databases (39) using one type of human GABA transporter (SLC6A1) (40) as a query identified several amino acid sequences of the neurotransmitter transporter SLC6A family. For the SLC6A family, the cDNAs of transporters expressed in various tissues were isolated. We then examined the accumulation of ALA-induced protoporphyrin by the expression of SLC6A6, SLC6A8, SLC6A12 and SLC6A13. These expressions were confirmed by immunoblotting with myc-tag antibody (Fig. 4A). The amount of protoporphyrin in the SLC6A6-, SLC6A8-, and SLC6A13-expressing HEK293T cells was much higher than that in control cells (Fig. 4B). SLC6A12 had no effect on the accumulation. When the cells expressing SLC6A transporters were also incubated with ALA-methylester, protoporphyrin accumulated more in SLC6A6-, SLC6A8- and SLC6A13-expressing cells than in control cells (Fig. 4C). The difference between the control and

transfectants in terms of protoporphyrin formation from ALA-methylester was much greater than in the case with ALA. We next examined the uptake of ALA by SLC6A6 or SLC6A13 cDNA-transfected HEK cells. The uptake of ALA by the cells increased in a manner dependent on incubation time. HEK cells expressing SLC6A6 and SLC6A13 could take up ALA at 2.5- and 4.5-fold higher than control cells, respectively (Fig. 5A).

To examine the photo-damage of the HEK cells, they were treated with 100-500 μM ALA for 6 h and then exposed to visible light. The death of the empty vector-transfected control cells was dependent on the dose of ALA (Fig. 5B). The cell death occurred as necrosis by the short-term irradiation, followed by the short-time incubation, and was evaluated as photo-toxicity. In addition, immunoblot analysis revealed that the cleavage of caspase-3 to the active form in the protophyrin-accumulated cells was not observed upon exposure to the light (data not shown), indicating that the apoptosis was not induced. SLC6A family transporter-expressing cells became more sensitive to the light than the control cells. These results indicated that the expression of SLC6A family transporters led to increase in the uptake of ALA by the cells and ALA-induced photo-damage.

Knockdown of SLC6A6 and SLC6A13 in DLD-1 and HeLa cells decreased the accumulation of ALA-induced protoporphyrin

We next examined whether knockdown of the expression of SLC6A6 or SLC6A13 with siRNA in DLD-1 and HeLa cells affects the ALA-induced accumulation of protoporphyrin. Immunoblot analysis confirmed the decrease of SLC6A6 and SLC6A13 in the knockdown cells. The accumulation in SLC6A6-deficient DLD-1 and HeLa cells was decreased to 80% and 65% of that of control cells, respectively (Fig. 6A,C). The reduced expression of SLC6A13 led to the decline of the ALA-induced accumulation of protoporphyrin through the lowered expression of the transporter (Fig. 6B,D).

Expression of SLC6A family transporters in human cancerous cells and colon cancer

It is known that neurotransmitter transporters SLC6A6 and SLC6A13 are abundant in nervous system. In addition, SLC6A6 is also expressed prominently in retina, skin, heart, breast, placenta and kidney (41, 42), and SLC6A13 is in prostate (43, 44) at mRNA level. Figure 5 shows the results of the expression of two transporters in human cell lines. SLC6A6 was found in human embryonic kidney HEK293, melanoma A375, glioblastoma T98G and colon cancer HCT116 cells, but not in Burkitt's lymphoma Daudi, T-cell leukemia Jurkat or rhabdomyosarcoma Rh30 cells. SLC6A13 was widely expressed in all cells, and especially highly expressed in HEK293, A375, T98G and epidermoid cancer Hep-2 cells. SLC6A8 was not found in any cell lines (data not shown). These results indicated that the two transporters were expressed differently among various tumor cells. Immunohistochemical staining was finally performed on 10% formalin-fixed, paraffin-embedded tumor tissue sections. As shown in Fig. 6, immunohistochemical staining with anti-SLC6A6 or anti-SLC6A13 revealed that SLC6A6 and SLC6A13 were clearly found in adenocarcinoma cells in the same specimen. However,

the normal epithelial cells were weakly or hardly stained for SLC6A6. The intensity of staining of SLC6A13 in normal epithelial cells was much less than that in tumor cells.

Discussion

The present study first demonstrated that Na^+- and Cl^--dependent neurotransmitter transporters of the SLC6A family are involved in the uptake of ALA by cancerous cells. Based on the results from the inhibition of the accumulation of protoporphyrin by GABA-related chemicals, including β-alanine and taurine in colon cancer DLD-1 cells, BLAST search with the amino acid sequence of GABA transporter SLC6A1 as a query showed high homologies to several Na^+- and Cl^--dependent neurotransmitter transporters of the SLC6A family. The expression of taurine transporter SLC6A6, creatine transporter SLC6A8 and GABA transporter SLC6A13 in HEK cells markedly enhanced the ALA-induced formation of protoporphyrin and photo-damage. However, the expression of betaine/GABA transporter SLC6A12 did not stimulate the accumulation. These results suggested that multiple neurotransmitter and amino acid transporters could be involved in the transport of ALA. Although most of these transporters were limitedly expressed in neuronal tissues, GABA-homologue transporters including SLC6A6 and SLC6A13 have been shown to be expressed in many tissues outside the central nervous system (45-48). Although the regulation of the expression of SLC6A6 and SLC6A13 in cancer cell lines remains unclear, taurine, transported by SLC6A6, was found to be essential for cell survival and development, which may contribute to dominant proliferation of tumors (49-51). SLC6A13 also plays a role of an import gateway of taurine into cancer cell lines (52, 53).

It is known that lipophilic ALA derivatives including ALA hexylester and ALA methylester improved the detection rate of both flat and papillary lesions in the imaging of bladder tumors (54). ALA-methylester based PDT is now considered to show high efficacy and safety (55). The uptake mechanism of ALA and its derivatives may differ in different types of cell although these are apparently incorporated into the neural cells through the same GABA transporters (56). The present data show that the incubation of cells with ALA-methylester resulted in a marked increase in the accumulation of protoporphyrin by the expression of SLC6A6, SLC6A8 and SLC6A13, suggesting more efficient uptake of ALA-methylester by these transporters. This is inconsistent with some preceding studies (29, 30, 57) on the ineffectiveness of ALA-methylester on the taking up of ALA and GABA by adenocarcinoma cells, and the ALA-induced accumulation of protoporphyrin. Rodriguez et al. (57) pointed out the difference of the attenuation between ester forms of ALA and substrates of neurotransmitter transporters in the uptake of ALA. However, there has been no direct assessment on specific transporters. Moreover, by homology modeling, namely, substrate binding site as well as docking scores, Baglo et al. (58) suggested that alkylesters of ALA may be substrates in GAT-2 (SLC6A13). Since the ester form of ALA is more hydrophobic than ALA, ALA esters can be taken

up easily into cells (59, 60). The present data demonstrated that SLC6A family is involved in both ALA methylester as well as ALA, suggesting that high efficiency on the accumulation of protoporphyrin by ALA methylester can be derived from preferential association to the cell membrane due to the hydrophobicity of the ester form of ALA. In addition, since multiple transporters can mediate uptake of ALA and its ester forms (29, 30), it is possible that additional transporters expressed in different types of cancerous cells can transport these compounds. In anyway, as far as the uptake of ALA methylester is concerned, we suggest that the uptake of the more lipophilic ALA derivatives should be further investigated, despite of its extensive clinical applications.

The inhibitory effect of GABA homologues on the ALA-induced accumulation of protoporphyrin in HeLa cells was less than that seen in the case of DLD-1 cells. The knockdown of SLC6A13 in HeLa cells led to a decrease of the level of protoporphyrin by a small amount, suggesting that other transporters play a major role in the transport of ALA. GABA transporter showed a structure similar to Na^+- and Cl^--dependent neutral and basic amino acid transporters. Neoplastic cells exhibit increased demands for certain metabolites including amino acids and adapt to this requirement by not only the enhanced expression of amino acid transporters but also in the expression of isoforms not found in normal tissues (61). Based on the overlapping specificities of amino acid and neurotransmitter transporters, the enhanced expression of amino acid transporters may account for more accumulation of protoporphyrin in various cancerous cells, including HeLa cells treated with ALA, than in normal cells.

The present study showed that ALA-induced accumulation of protoporphyrin was not enhanced by the expression of SLC6A12. The reason about no effect is unclear, but it is possible that the affinity for ALA is not so high or some unknown factors are required for the transport since SLC6A12 acts as a betaine transporter. In this connection, Bermudez Moretti et al. (62) reported that ALA uptake by cells is strongly inhibited by GABA, β-alanine and taurine, while betaine was without effect. These observations may explain the ineffectiveness of SLC6A12 on the accumulation of protoporphyrin. In addition to the role of SLC6A family transporters in the uptake of ALA by cells, other investigators reported that ALA was a substrate of the H^+-coupled amino acid transporter PAT1 (SLC36A1) after heterologous expression in *Xenopus laevi*s oocytes (12) and in Cos7 cells (13). Intestinal transport of ALA was also mediated by the apical dipeptide transporters PEPT1 (SLC15A1) and PEPT2 (SLC15A2). PEPT1 is only present in intestinal tissues and its mRNA was found to be increased in colon cancer tissues, but not PAT1 or PEPT2 (12), suggesting that selective accumulation of protoporphyrin in colon cancer can be due to increased uptake of ALA by PEPT1. Thus, the combination of SLC6A family and PEPT1 in the transport of ALA and dysfunction of p53 causing mitochondrial iron utilization for heme biosynthesis (9) in cancerous cells contributes to synergistic augmentation of the accumulation of protoporphyrin.

Silencing of SLC6A6 and SLC6A13 proteins leading to a reduction of the amount of photosensitizer induced by ALA (Fig. 5A) indicates their presence and participation in PDT. In particular, the most predominant effect of SLC6A6 in human colorectal adenocarcinoma DLD-1 cells, in combination with its expression in colon cancer HCT116 cells positively detected by immunoblotting (Fig. 4), indicated that these transporters can become good markers of colon cancer. Alternatively, immunohistochemical observations with the antibodies for the transporters (Fig. 6) hold promise as a powerful application of PDT in treatment colorectal tumors, which ranks as the third most common cancer worldwide and account for over 9% of total cancer incidence (63). These findings have led some authors to suggest that, in particular, neurotransmitter transporters are involved in ALA transport in colon adenocarcinoma cells (29) or, in general, preferential accumulation of protoporphyrin in mucosa by ALA-PDT might be favorable in the treatment of gastrointestinal cancers (64). Besides, regarding to SLC6A13 transporter, examinations on this resulted in analogous outcomes as compared with the SLC6A6. In addition, the presence of this GABA transporter in all cell lines investigated suggests its potential for wide application of it in oncology.

Finally, another issue relating to both ALA and GABA is pain, associated with and also a limiting factor of ALA-induced PDT, especially in skin treatment. GABA is a novel neurotransmitter located in peripheral neurons (65, 66). Therefore, its transporters' ALA uptake ability may explain the penetrating of this substance into nerve endings, which causing the side effect mentioned. This was mentioned by Rud et al. and Baglo et al., as well (29, 58). With the predominant affect in both taking up ALA and enhancing protoporphyrin IX accumulation in the present study, SLC6A13, with the main substrate GABA, could play either the accelerator of consuming ALA for a more efficient therapy or the better control of pain as well as improving this drawback of ALA-based PDT, in addition to current strategies including desensitizing the nerves, blocking nerve depolarization or attempting to minimize protoporphyrin accumulation in nerve endings (67). In several clinical trials, ALA has been reported to cause greater sufferings than the methylester form (68, 69). Thus far, in combination with the obtained higher efficiency of forming protoporphyrin from ALA-methylester uptake, it suggests that the pain drawback comes from nature of the prodrugs, namely from their interaction with establishment of sensation, other than the photosensitizer accumulation. This modality was suggested by Wiegell et al. before (69). Thus, the mechanisms relating to this issue are obviously essential to be clarified in order to complete pain-relief solutions.

References

1. Dougherty, T. J. (1984) Photodynamic therapy (PDT) of malignant tumors. *Crit Rev Oncol Hematol* **2**, 83-116.

2. Feuerstein, T., G. Berkovitch-Luria, A. Nudelman, A. Rephaeli and Z. Malik (2011) Modulating ALA-PDT efficacy of mutlidrug resistant MCF-7 breast cancer cells using ALA prodrug. *Photochem Photobiol Sci* **10**, 1926-33.

3. Hirschberg, H., F. A. Uzal, D. Chighvinadze, M. J. Zhang, Q. Peng and S. J. Madsen (2008) Disruption of the blood-brain barrier following ALA-mediated photodynamic therapy. *Lasers Surg Med* **40**, 535-42.

4. Dougherty, T. J., C. J. Gomer, B. W. Henderson, G. Jori, D. Kessel, M. Korbelik, J. Moan and Q. Peng (1998) Photodynamic therapy. *J Natl Cancer Inst* **90**, 889-905.

5. Ohgari, Y., Y. Miyata, T. Miyagi, S. Gotoh, T. Ohta, T. Kataoka, K. Furuyama and S. Taketani (2011) Roles of porphyrin and iron metabolisms in the delta-aminolevulinic acid (ALA)-induced accumulation of protoporphyrin and photodamage of tumor cells. *Photochem Photobiol* **87**, 1138-45.

6. Stummer, W., S. Stocker, A. Novotny, A. Heimann, O. Sauer, O. Kempski, N. Plesnila, J. Wietzorrek and H. J. Reulen (1998) In vitro and in vivo porphyrin accumulation by C6 glioma cells after exposure to 5-aminolevulinic acid. *J Photochem Photobiol B* **45**, 160-9.

7. Ohgari, Y., Y. Nakayasu, S. Kitajima, M. Sawamoto, H. Mori, O. Shimokawa, H. Matsui and S. Taketani (2005) Mechanisms involved in delta-aminolevulinic acid (ALA)-induced photosensitivity of tumor cells: relation of ferrochelatase and uptake of ALA to the accumulation of protoporphyrin. *Biochem Pharmacol* **71**, 42-9.

8. Teng, L., M. Nakada, S. G. Zhao, Y. Endo, N. Furuyama, E. Nambu, I. V. Pyko, Y. Hayashi and J. I. Hamada (2011) Silencing of ferrochelatase enhances 5-aminolevulinic acid-based fluorescence and photodynamic therapy efficacy. *Br J Cancer* **104**, 798-807.

9. Sawamoto, M., T. Imai, M. Umeda, K. Fukuda, T. Kataoka and S. Taketani (2013) The p53-dependent expression of frataxin controls 5-aminolevulinic acid-induced accumulation of protoporphyrin IX and photo-damage in cancerous cells. *Photochem Photobiol* **89**, 163-72.

10. Kristensen, A. S., J. Andersen, T. N. Jorgensen, L. Sorensen, J. Eriksen, C. J. Loland, K. Stromgaard and U. Gether (2011) SLC6 neurotransmitter transporters: structure, function, and regulation. *Pharmacol Rev* **63**, 585-640.

11. Schauder, A., T. Feuerstein and Z. Malik (2011) The centrality of PBGD expression levels on ALA-PDT efficacy. *Photochem Photobiol Sci* **10**, 1310-7.

12. Anderson, C. M., M. Jevons, M. Thangaraju, N. Edwards, N. J. Conlon, S. Woods, V. Ganapathy and D. T. Thwaites (2010) Transport of the photodynamic therapy agent 5-aminolevulinic acid by distinct H+-coupled nutrient carriers coexpressed in the small intestine. *J Pharmacol Exp Ther* **332**, 220-8.

13. Frolund, S., O. C. Marquez, M. Larsen, B. Brodin and C. U. Nielsen (2010) Delta-aminolevulinic acid is a substrate for the amino acid transporter SLC36A1 (hPAT1). *Br J Pharmacol* **159**, 1339-53.

14. Rodriguez, L., A. Batlle, G. Di Venosa, A. J. MacRobert, S. Battah, H. Daniel and A. Casas (2006) Study of the mechanisms of uptake of 5-aminolevulinic acid derivatives by PEPT1 and PEPT2 transporters as a tool to improve photodynamic therapy of tumours. *Int J Biochem Cell Biol* **38**, 1530-9.

15. Christensen, H. N., M. Liang and E. G. Archer (1967) A distinct Na+-requiring transport system for alanine, serine, cysteine, and similar amino acids. *J Biol Chem* **242**, 5237-46.

16. Utsunomiya-Tate, N., H. Endou and Y. Kanai (1996) Cloning and functional characterization of a system ASC-like Na+-dependent neutral amino acid transporter. *J Biol Chem* **271**, 14883-90.

17. Arriza, J. L., M. P. Kavanaugh, W. A. Fairman, Y. N. Wu, G. H. Murdoch, R. A. North and S. G. Amara (1993) Cloning and expression of a human neutral amino acid transporter with structural similarity to the glutamate transporter gene family. *J Biol Chem* **268**, 15329-32.

18. Shafqat, S., B. K. Tamarappoo, M. S. Kilberg, R. S. Puranam, J. O. McNamara, A. Guadano-Ferraz and R. T. Fremeau, Jr. (1993) Cloning and expression of a novel Na(+)-dependent neutral amino acid transporter structurally related to mammalian Na+/glutamate cotransporters. *J Biol Chem* **268**, 15351-5.

19. Kanai, Y. (1997) Family of neutral and acidic amino acid transporters: molecular biology, physiology and medical implications. *Curr Opin Cell Biol* **9**, 565-72.

20. Mackenzie, B. and J. D. Erickson (2004) Sodium-coupled neutral amino acid (System N/A) transporters of the SLC38 gene family. *Pflugers Arch* **447**, 784-95.

21. Gu, S., C. J. Villegas and J. X. Jiang (2005) Differential regulation of amino acid transporter SNAT3 by insulin in hepatocytes. *J Biol Chem* **280**, 26055-62.

22. Boulland, J. L., K. K. Osen, L. M. Levy, N. C. Danbolt, R. H. Edwards, J. Storm-Mathisen and F. A. Chaudhry (2002) Cell-specific expression of the glutamine transporter SN1 suggests differences in dependence on the glutamine cycle. *Eur J Neurosci* **15**, 1615-31.

23. Boulland, J. L., A. Rafiki, L. M. Levy, J. Storm-Mathisen and F. A. Chaudhry (2003) Highly differential expression of SN1, a bidirectional glutamine transporter, in astroglia and endothelium in the developing rat brain. *Glia* **41**, 260-75.

24. Varoqui, H. and J. D. Erickson (2002) Selective up-regulation of system a transporter mRNA in diabetic liver. *Biochem Biophys Res Commun* **290**, 903-8.

25. Gu, S., H. L. Roderick, P. Camacho and J. X. Jiang (2000) Identification and characterization of an amino acid transporter expressed differentially in liver. *Proc Natl Acad Sci U S A* **97**, 3230-5.

26. Chaudhry, F. A., R. J. Reimer, D. Krizaj, D. Barber, J. Storm-Mathisen, D. R. Copenhagen and R. H. Edwards (1999) Molecular analysis of system N suggests novel physiological roles in nitrogen metabolism and synaptic transmission. *Cell* **99**, 769-80.

27. Sato, H., M. Tamba, T. Ishii and S. Bannai (1999) Cloning and expression of a plasma membrane

cystine/glutamate exchange transporter composed of two distinct proteins. *J Biol Chem* **274**, 11455-8.

28. Wang, H., M. Tamba, M. Kimata, K. Sakamoto, S. Bannai and H. Sato (2003) Expression of the activity of cystine/glutamate exchange transporter, system x(c)(-), by xCT and rBAT. *Biochem Biophys Res Commun* **305**, 611-8.

29. Rud, E., O. Gederaas, A. Hogset and K. Berg (2000) 5-aminolevulinic acid, but not 5-aminolevulinic acid esters, is transported into adenocarcinoma cells by system BETA transporters. *Photochem Photobiol* **71**, 640-7.

30. Gederaas, O. A., A. Holroyd, S. B. Brown, D. Vernon, J. Moan and K. Berg (2001) 5-Aminolaevulinic acid methyl ester transport on amino acid carriers in a human colon adenocarcinoma cell line. *Photochem Photobiol* **73**, 164-9.

31. Tomokuni, K. and M. Ogata (1972) Simple method for determination of urinary -aminolevulinic acid as an index of lead exposure. *Clin Chem* **18**, 1534-8.

32. Di Venosa, G., C. Perotti, H. Fukuda, A. Batlle and A. Casas (2005) Sensitivity to ALA-PDT of cell lines with different nitric oxide production and resistance to NO cytotoxicity. *J Photochem Photobiol B* **80**, 195-202.

33. Wild, P. J., R. C. Krieg, J. Seidl, R. Stoehr, K. Reher, C. Hofmann, J. Louhelainen, A. Rosenthal, A. Hartmann, C. Pilarsky, A. K. Bosserhoff and R. Knuechel (2005) RNA expression profiling of normal and tumor cells following photodynamic therapy with 5-aminolevulinic acid-induced protoporphyrin IX in vitro. *Mol Cancer Ther* **4**, 516-28.

34. Frank, J., M. R. Lornejad-Schafer, H. Schoffl, A. Flaccus, C. Lambert and H. K. Biesalski (2007) Inhibition of heme oxygenase-1 increases responsiveness of melanoma cells to ALA-based photodynamic therapy. *Int J Oncol* **31**, 1539-45.

35. Ohgari, Y., Y. Miyata, T. T. Chau, S. Kitajima, Y. Adachi and S. Taketani (2011) Quinolone compounds enhance delta-aminolevulinic acid-induced accumulation of protoporphyrin IX and photosensitivity of tumour cells. *J Biochem* **149**, 153-60.

36. Beale, S. I., S. P. Gough and S. Granick (1975) Biosynthesis of delta-aminolevulinic acid from the intact carbon skeleton of glutamic acid in greening barley. *Proc Natl Acad Sci U S A* **72**, 2719-23.

37. Gough, S. P., S. I. Beale and S. Granick (1976) The biosynthesis of delta-aminolevulinic acid from the intact carbon skeleton of glutamic acid in greening barley. *Ann Clin Res* **8 Suppl 17**, 70-3.

38. Sawada, S., M. Higashima and C. Yamamoto (1985) Inhibitors of high-affinity uptake augment depolarizations of hippocampal neurons induced by glutamate, kainate and related compounds. *Exp Brain Res* **60**, 323-9.

39. Altschul, S. F., T. L. Madden, A. A. Schaffer, J. Zhang, Z. Zhang, W. Miller and D. J. Lipman (1997) Gapped BLAST and PSI-BLAST: a new generation of protein database search programs. *Nucleic Acids Res* **25**, 3389-402.

40. Nelson, H., S. Mandiyan and N. Nelson (1990) Cloning of the human brain GABA transporter. *FEBS Lett* **269**, 181-4.

41. Ramamoorthy, S., F. H. Leibach, V. B. Mahesh, H. Han, T. Yang-Feng, R. D. Blakely and V. Ganapathy (1994) Functional characterization and chromosomal localization of a cloned taurine transporter from human placenta. *Biochem J* **300 (Pt 3)**, 893-900.

42. Jhiang, S. M., L. Fithian, P. Smanik, J. McGill, Q. Tong and E. L. Mazzaferri (1993) Cloning of the human taurine transporter and characterization of taurine uptake in thyroid cells. *FEBS Lett* **318**, 139-44.

43. Gong, Y., M. Zhang, L. Cui and G. Y. Minuk (2001) Sequence and chromosomal assignment of a human novel cDNA: similarity to gamma-aminobutyric acid transporter. *Can J Physiol Pharmacol* **79**, 977-84.

44. Christiansen, B., A. K. Meinild, A. A. Jensen and H. Brauner-Osborne (2007) Cloning and characterization of a functional human gamma-aminobutyric acid (GABA) transporter, human GAT-2. *J Biol Chem* **282**, 19331-41.

45. Borden, L. A., K. E. Smith, P. R. Hartig, T. A. Branchek and R. L. Weinshank (1992) Molecular heterogeneity of the gamma-aminobutyric acid (GABA) transport system. Cloning of two novel high affinity GABA transporters from rat brain. *J Biol Chem* **267**, 21098-104.

46. Tiruppathi, C., M. Brandsch, Y. Miyamoto, V. Ganapathy and F. H. Leibach (1992) Constitutive expression of the taurine transporter in a human colon carcinoma cell line. *Am J Physiol* **263**, G625-31.

47. Matsuyama, S., N. Saito, K. Taniyama and C. Tanaka (1991) gamma-Aminobutyric acid is a neuromodulator in sinus node of guinea pig heart. *Am J Physiol* **261**, H1437-42.

48. Cutting, G. R., L. Lu, B. F. O'Hara, L. M. Kasch, C. Montrose-Rafizadeh, D. M. Donovan, S. Shimada, S. E. Antonarakis, W. B. Guggino, G. R. Uhl and et al. (1991) Cloning of the gamma-aminobutyric acid (GABA) rho 1 cDNA: a GABA receptor subunit highly expressed in the retina. *Proc Natl Acad Sci U S A* **88**, 2673-7.

49. Ito, T., Y. Fujio, Y. Uozumi, T. Matsuda, M. Maeda, K. Takahashi and J. Azuma (2006) TauT gene expression is regulated by TonEBP and plays a role in cell survival. *Adv Exp Med Biol* **583**, 91-8.

50. Li, Y., J. M. Arnold, M. Pampillo, A. V. Babwah and T. Peng (2009) Taurine prevents cardiomyocyte death by inhibiting NADPH oxidase-mediated calpain activation. *Free Radic Biol Med* **46**, 51-61.

51. Ito, T., Y. Kimura, Y. Uozumi, M. Takai, S. Muraoka, T. Matsuda, K. Ueki, M. Yoshiyama, M. Ikawa, M. Okabe, S. W. Schaffer, Y. Fujio and J. Azuma (2008) Taurine depletion caused by knocking out the taurine transporter gene leads to cardiomyopathy with cardiac atrophy. *J Mol Cell Cardiol* **44**, 927-37.

52. Zhou, Y., S. Holmseth, C. Guo, B. Hassel, G. Hofner, H. S. Huitfeldt, K. T. Wanner and N. C. Danbolt (2012) Deletion of the gamma-aminobutyric acid transporter 2 (GAT2 and SLC6A13) gene in mice leads to changes in liver and brain taurine contents. *J Biol Chem* **287**, 35733-46.

53. Ikeda, S., M. Tachikawa, S. Akanuma, J. Fujinawa and K. Hosoya (2012) Involvement of gamma-aminobutyric acid transporter 2 in the hepatic uptake of taurine in rats. *Am J Physiol Gastrointest Liver*

Physiol **303**, G291-7.

54. Schmidbauer, J., F. Witjes, N. Schmeller, R. Donat, M. Susani, M. Marberger and P. C. B. S. G. Hexvix (2004) Improved detection of urothelial carcinoma in situ with hexaminolevulinate fluorescence cystoscopy. *J Urol* **171**, 135-8.

55. Dirschka, T., P. Radny, R. Dominicus, H. Mensing, H. Bruning, L. Jenne, L. Karl, M. Sebastian, C. Oster-Schmidt, W. Klovekorn, U. Reinhold, M. Tanner, D. Grone, M. Deichmann, M. Simon, F. Hubinger, G. Hofbauer, G. Krahn-Senftleben, F. Borrosch, K. Reich, C. Berking, P. Wolf, P. Lehmann, M. Moers-Carpi, H. Honigsmann, K. Wernicke-Panten, C. Helwig, M. Foguet, B. Schmitz, H. Lubbert, R. M. Szeimies and A.-C. S. Group (2012) Photodynamic therapy with BF-200 ALA for the treatment of actinic keratosis: results of a multicentre, randomized, observer-blind phase III study in comparison with a registered methyl-5-aminolaevulinate cream and placebo. *Br J Dermatol* **166**, 137-46.

56. Novak, B., R. Schulten and H. Lubbert (2011) delta-Aminolevulinic acid and its methyl ester induce the formation of Protoporphyrin IX in cultured sensory neurones. *Naunyn Schmiedebergs Arch Pharmacol* **384**, 583-602.

57. Rodriguez, L., A. Batlle, G. Di Venosa, S. Battah, P. Dobbin, A. J. Macrobert and A. Casas (2006) Mechanisms of 5-aminolevulinic acid ester uptake in mammalian cells. *Br J Pharmacol* **147**, 825-33.

58. Baglo, Y., M. Gabrielsen, I. Sylte and O. A. Gederaas (2013) Homology modeling of human gamma-butyric acid transporters and the binding of pro-drugs 5-aminolevulinic acid and methyl aminolevulinic acid used in photodynamic therapy. *PLoS One* **8**, e65200.

59. Kloek, J. and H. Beijersbergen van (1996) Prodrugs of 5-aminolevulinic acid for photodynamic therapy. *Photochem Photobiol* **64**, 994-1000.

60. Brunner, H., F. Hausmann, R. C. Krieg, E. Endlicher, J. Scholmerich, R. Knuechel and H. Messmann (2001) The effects of 5-aminolevulinic acid esters on protoporphyrin IX production in human adenocarcinoma cell lines. *Photochem Photobiol* **74**, 721-5.

61. McGivan, J. D. (1998) Rat hepatoma cells express novel transport systems for glutamine and glutamate in addition to those present in normal rat hepatocytes. *Biochem J* **330 (Pt 1)**, 255-60.

62. Bermudez Moretti, M., S. Correa Garcia, C. Perotti, A. Batlle and A. Casas (2002) Delta-Aminolevulinic acid transport in murine mammary adenocarcinoma cells is mediated by beta transporters. *Br J Cancer* **87**, 471-4.

63. Haggar, F. A. and R. P. Boushey (2009) Colorectal cancer epidemiology: incidence, mortality, survival, and risk factors. *Clin Colon Rectal Surg* **22**, 191-7.

64. Wachowska, M., A. Muchowicz, M. Firczuk, M. Gabrysiak, M. Winiarska, M. Wańczyk, K. Bojarczuk and J. Golab (2011) Aminolevulinic Acid (ALA) as a Prodrug in Photodynamic Therapy of Cancer. *Molecules* **16**, 4140-64.

65. Krantis, A. and T. Webb (1989) Autoradiographic localization of [3H] gamma-aminobutyric acid in

neuronal elements of the rat gastric antrum and intestine. *J Auton Nerv Syst* **29**, 41-8.

66. Tillakaratne, N. J., L. Medina-Kauwe and K. M. Gibson (1995) gamma-Aminobutyric acid (GABA) metabolism in mammalian neural and nonneural tissues. *Comp Biochem Physiol A Physiol* **112**, 247-63.

67. Warren, C. B., L. J. Karai, A. Vidimos and E. V. Maytin (2009) Pain associated with aminolevulinic acid-photodynamic therapy of skin disease. *J Am Acad Dermatol* **61**, 1033-43.

68. Moloney, F. J. and P. Collins (2007) Randomized, double-blind, prospective study to compare topical 5-aminolaevulinic acid methylester with topical 5-aminolaevulinic acid photodynamic therapy for extensive scalp actinic keratosis. *Br J Dermatol* **157**, 87-91.

69. Wiegell, S. R., I. M. Stender, R. Na and H. C. Wulf (2003) Pain associated with photodynamic therapy using 5-aminolevulinic acid or 5-aminolevulinic acid methylester on tape-stripped normal skin. *Arch Dermatol* **139**, 1173-7.

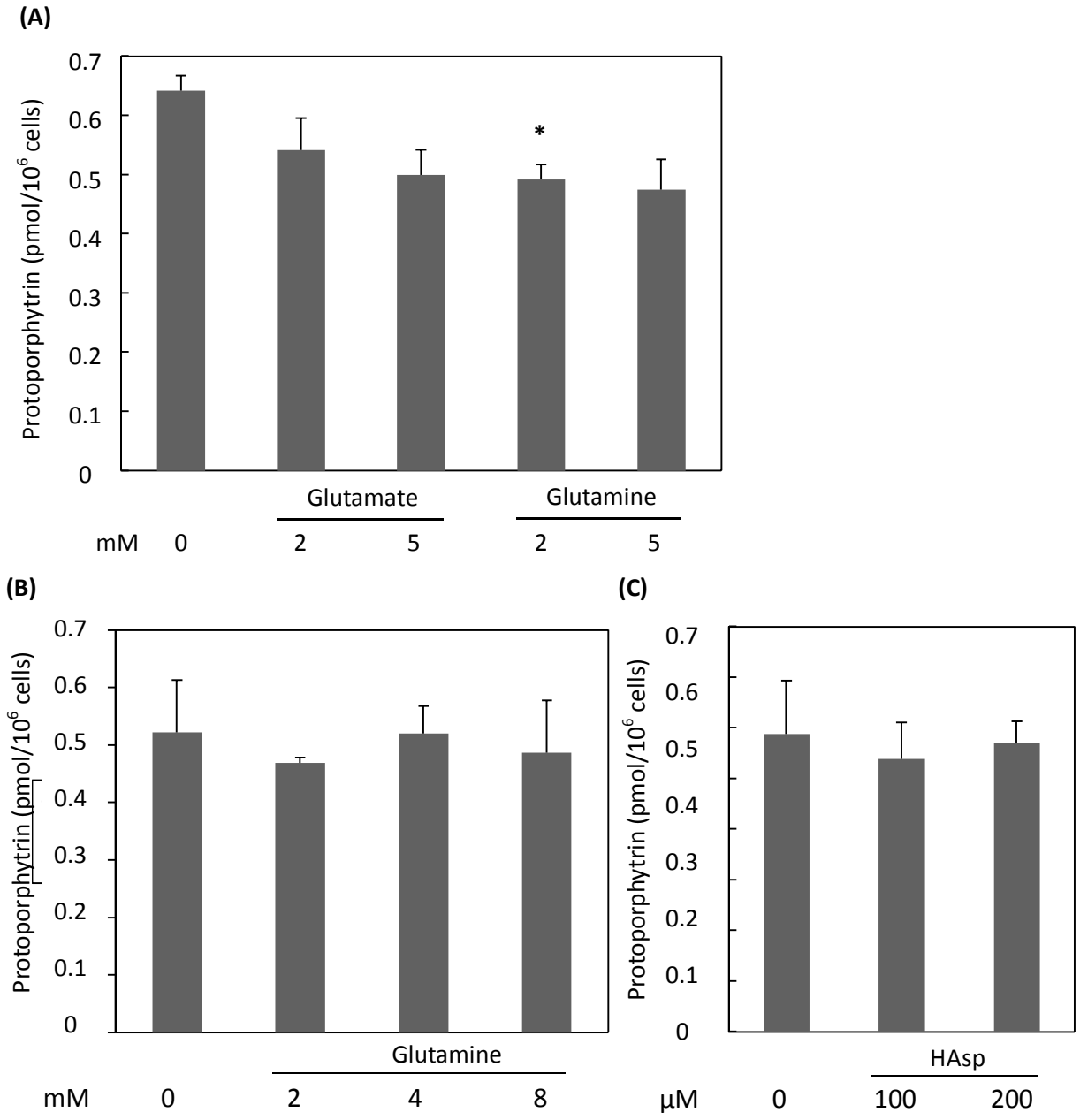

Figure 1. Effect of glutamine and glutamate on the ALA-induced accumulation of protoporphyrin in cancerous cells. (A) HeLa cells were incubated with the indicated inhibitors and 500 μM ALA for 4 h. (B) HeLa cells were incubated with the indicated concentration of glutamine and 500 μM ALA for 4 h. (C) HeLa cells were incubated with the indicated concentration of HAsp and 500 μM ALA for 4 h. Porphyrin was extracted from the cells and measured using a fluorospectrophotometer. Data are expressed as the mean ± S.D. of 4 independent experiments. Two-sample t-test was carried out: *, vs. ALA alone.

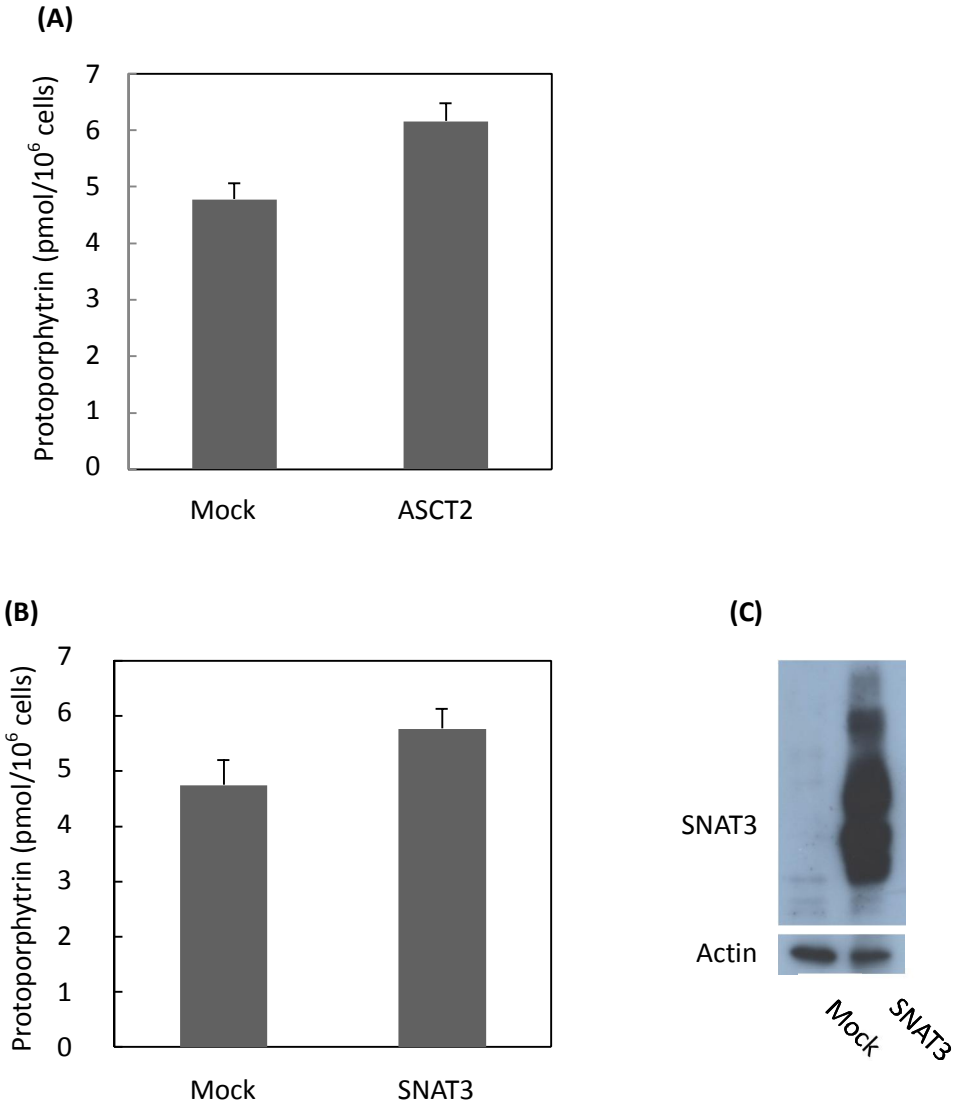

Figure 2. Effect of glutamine-transporters expression on ALA-induced protoporphyrin accumulation and photo-damage in HEK293T cells. Effect of the expression of ASCT2 (A) and SNAT3 (B) on the ALA-induced accumulation of protoporphyrin. HEK cells (5×10^5) transfected with the indicated plasmids were incubated for 24 h and treated with 500 μM ALA for 4 h. The cells were washed twice with phosphate-buffered saline, and then porphyrin was extracted and measured fluorospectrophotometrically. Data are expressed as the mean ± S.D. of 4 experiments. *, $P<0.01$ and **, $P<0.05$. (C) Immunoblot analysis. HEK293T cells were transfected with pcDNA3.1-myc-SNAT3. After 16 h of incubation, cell lysates from the cells were prepared. Cellular proteins were analyzed by SDS-PAGE, followed by immunoblotting with anti-myc-tag and anti-actin antibodies.

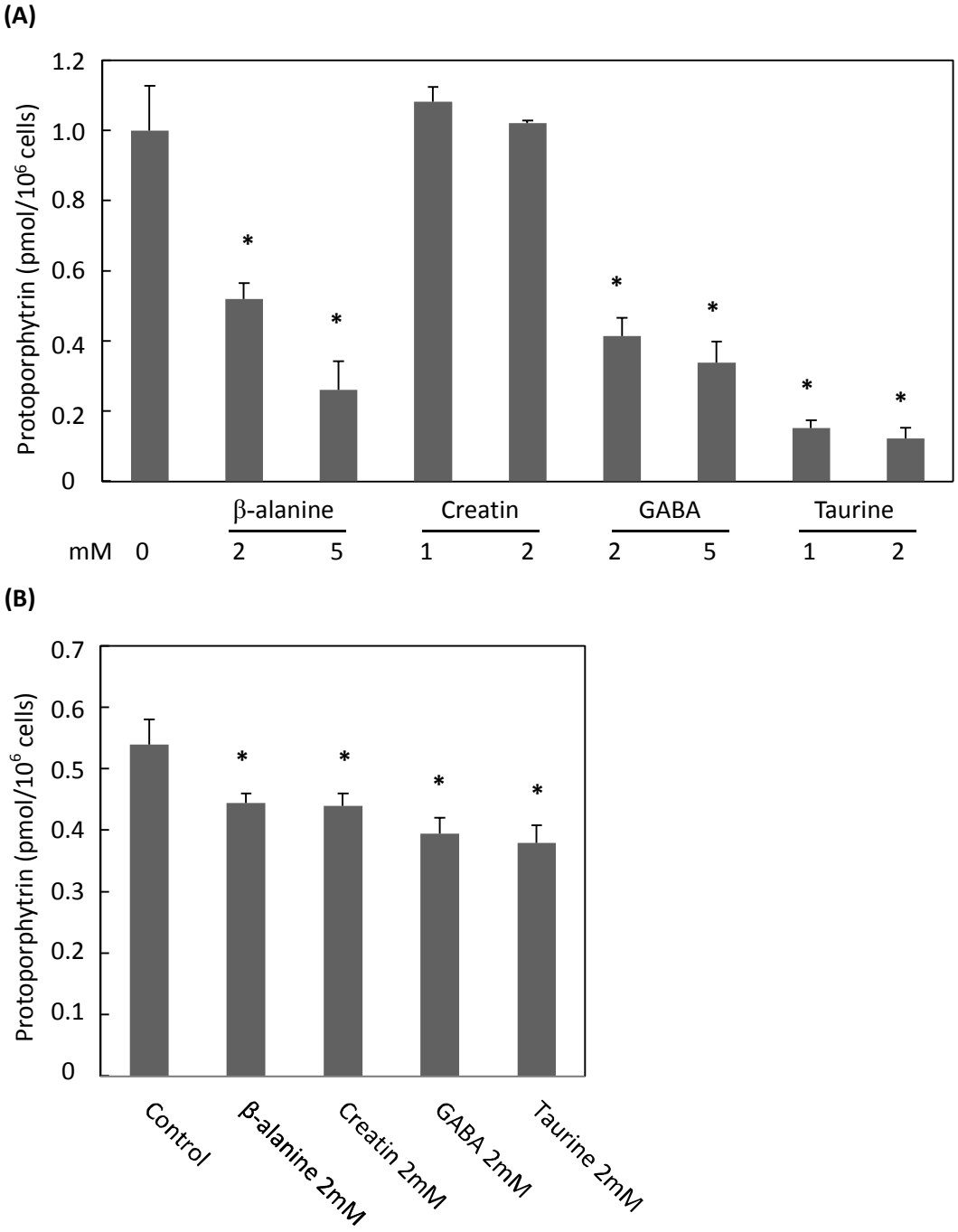

Figure 3. Effect of β-alanine, creatine, GABA and taurine on the ALA-induced accumulation of protoporphyrin in cancerous cells. DLD-1 (A) and HeLa cells (B) were incubated with the indicated inhibitors and 500 μM ALA for 4 h. Porphyrin was extracted from the cells and measured using a fluorospectrophotometer. Data are expressed as the mean ± S.D. of 4 independent experiments. Two-sample t-test was carried out: *, $P<0.01$ and **, $P<0.05$ vs. ALA alone.

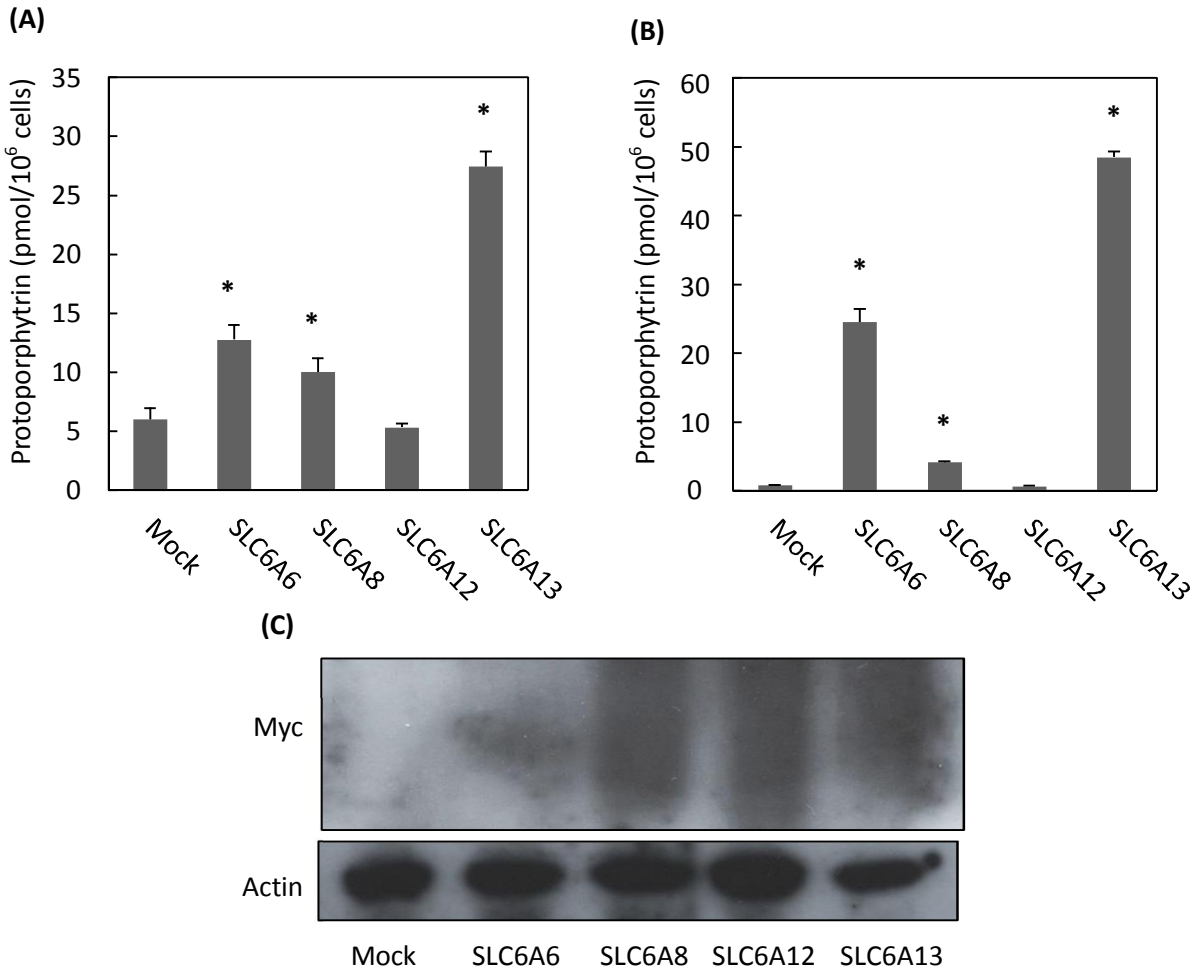

Figure 4. Effect of expression of the neurotransmitter transporter SLC6A family on ALA-induced protoporphyrin accumulation and photo-damage in HEK293T cells. (A) Immunoblot analysis. HEK293T cells were transfected with pcDNA3.1-myc-SLC6A6, pcDNA3-myc-SLC6A8, pcDNA3.1-myc-SLC6A12 and pcDNA3.1-myc-SLC6A13. After 16 h of incubation, cell lysates from the cells were prepared. Cellular proteins were analyzed by SDS-PAGE, followed by immunoblotting with anti-myc-tag and anti-actin antibodies. (B) Effect of the expression of SLC6A6, SLC6A8, SLC6A12 and SLC6A13 on the ALA-induced accumulation of protoporphyrin. HEK cells (5 x 10^5) transfected with the indicated plasmids were incubated for 24 h and treated with 500 μM ALA for 4 h. The cells were washed twice with phosphate-buffered saline, and then porphyrin was extracted and measured fluorospectrophotometrically. Data are expressed as the mean ± S.D. of 4 experiments. *, $P<0.01$ and **, $P<0.05$. (C) Effect of the expression of SLC6A6, SLC6A8, SLC6A12 and SLC6A13 on the ALA-methylester-induced accumulation of protoporphyrin. The transfection of the indicated plasmids and treatment of cells were similar to those described above, except for the addition of 1 mM ALA-methylester to the medium. *, $P<0.01$ and **, $P<0.05$.

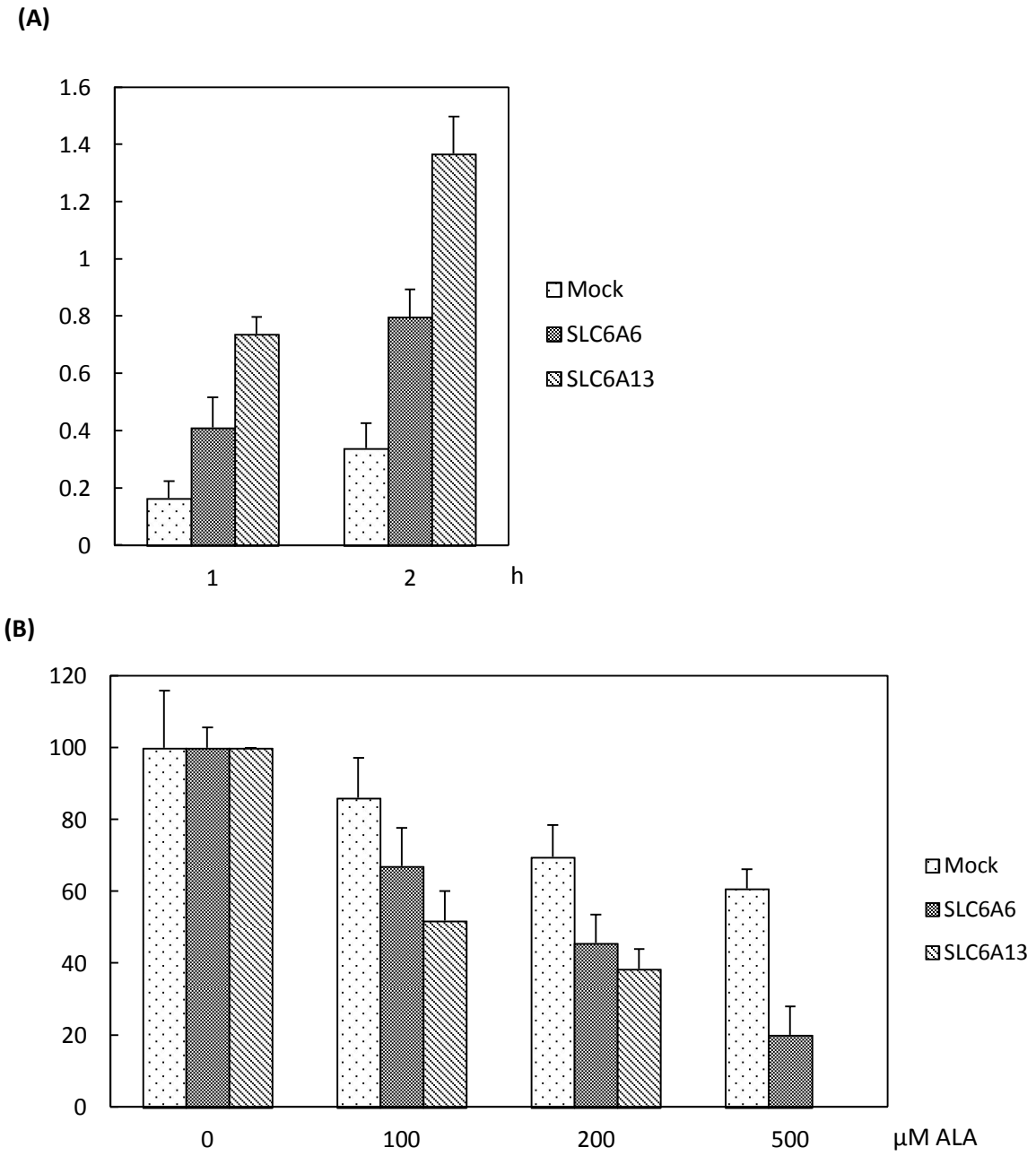

Figure 5. Effect of the expression of SLC6A6 and SLC6A13 on the uptake of ALA by HEK cells and the ALA-induced photodamage. (A) The uptake of ALA. HEK cells (5 x 10^5) transfected with plasmids carrying SLC6A6 and SLC6A13 were incubated for 24 h and treated with 20 μM ALA. At the indicated time, aliquots of culture medium were withdrawn. The amount of ALA in the medium was determined by spectrophotometry, as described. Data are expressed as mean ± S.D. of 6 experiments. *, $P<0.01$. (B) Photosensitivity. The transfected cells were incubated and fresh DMEM was added to the cells treated with 100-500 μM ALA for 6 h, followed by exposure to white light of fluorescence lamp for 10 min with dose 0.81 J/cm^2, and then surviving cells after no exposure or exposure to light were assessed by MTT assay. Data are the mean ± S.D. of 3 independent experiments.

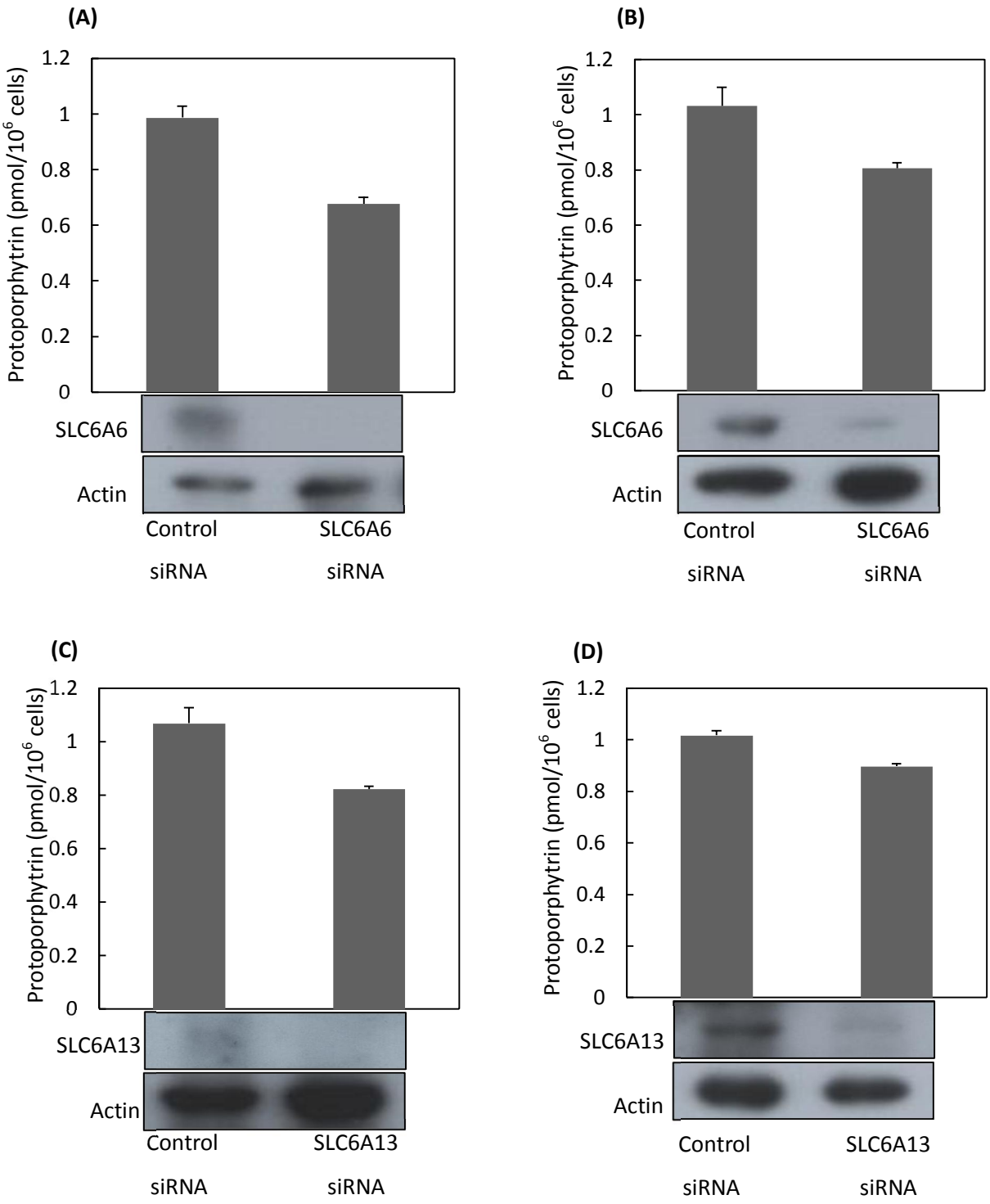

Figure 6. The decrease of the ALA-induced accumulation of protoporphyrin by knockdown of SLC6A6 and SLC6A13. The DLD-1 (A) and HeLa (B) cells transfected with control and SLC6A6 siRNA were incubated for 48 h, followed by incubation with 500 μM ALA for 4 h. The accumulation of protoporphyrin in the cells was estimated. *, $P<0.01$ and **, $p<0.05$ versus control. The knockdown of SLC6A13 was also carried out with DLD-1 (C) and HeLa (D) cells.

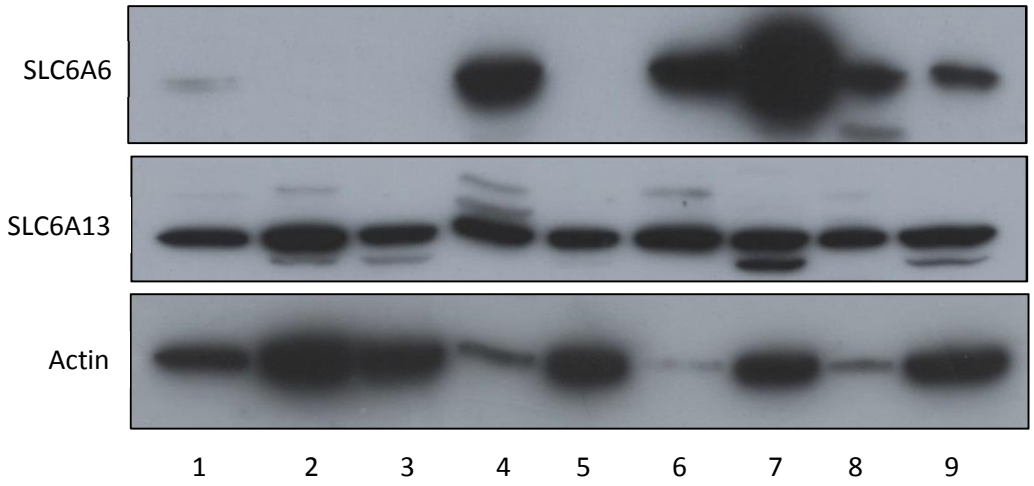

Figure 7. Expression of SLC6A6 and SLC6A13 in multiple human cells. Immunoblot analysis was carried out with anti-SLC6A6, anti-SLC6A13 and actin antibodies. (1) HeLa, (2) Jurkat, (3) Daudi, (4) HEK293T, (5) Rh30, (6) A375, (7) T98G, (8) HCT-116 and (9) Hep-2 cells.

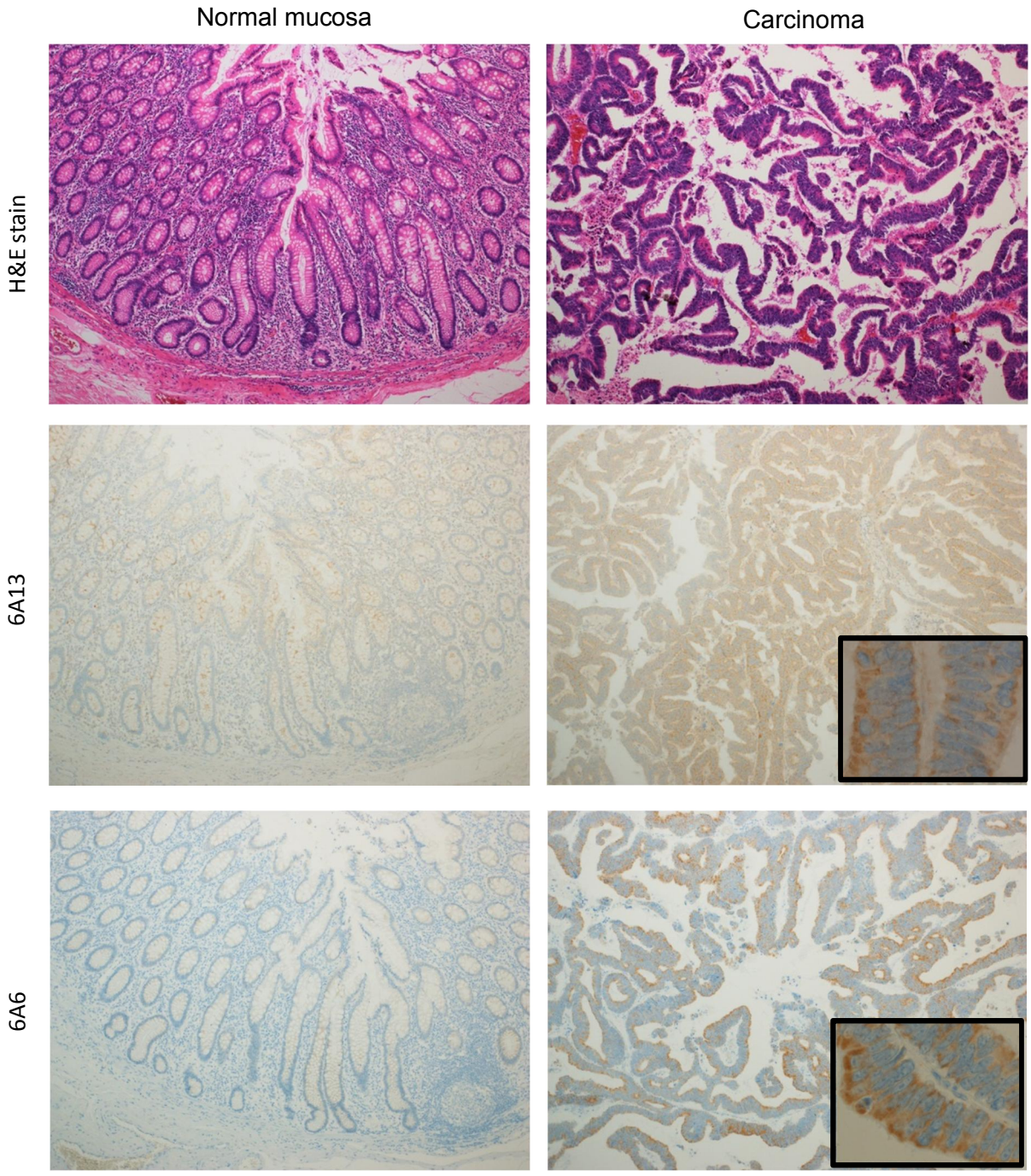

Figure 8. Hematoxylin & eosin staining, and immunohistochemistry staining with SLC6A6 and SLC6A13 antibodies of colon adenocarcinoma. Hematoxylin & eosin staining and immunohistochemistry staining with anti-SLC6A6 and anti-SLC66A13 antibodies of colon adenocarcinoma were carried out, as described in the Materials and Methods. Representative photos are shown (objective lens: x10 and x40 in the insets).

Chapter 2

p53 directly regulates the transcription of the human frataxin gene and its lack of regulation in tumor cells decreases the utilization of mitochondrial iron

Introduction

The mutation of homozygous expansion of a GAA trinucleotide repeat in intron 1 of the frataxin gene on chromosome 9q13 causes a defect of transcription (1). And lack of frataxin, a small mitochondrial protein, is the accepted cause of the entire complex clinical and pathological phenotype of FRDA. FRDA is a neurodegradative inherited disease, which includes abnormalities such as neurodegradation of large sensory neurons, cardiomyopathy, impaired glucose tolerance, and diabetes mellitus (2, 3). Hepatic-specific knockdown of the frataxin gene in mouse reduced the life span and caused tumor formation, which resemble the conditions of FRDA patients who suffer various types of cancer and reduced life span (4).

Regarding ALA-PDT, aside from the biosynthesis from ALA according to the heme forming pathway, protoporphyrin accumulation is regulated by the FECH activity (5). Frataxin is an iron-binding protein, contributing to the biogenesis of iron-sulfur clusters (6). The iron-sulfur cluster-containing proteins in mitochondria include the complex of the electron transport chain and FECH, the enzyme for the last step of heme biosynthesis (5). Besides, the expression of frataxin increased the mitochondrial function and decreased tumor-specific abnormality on the ALA-induced accumulation of protoporphyrin. The expression of frataxin was low in human cancer cells and the reduction of the function of frataxin in cancerous cells lead to the decrease of mitochondrial function including FECH and following photosensitizer accumulation in ALA-PDT (7).

The tumor suppressor protein p53 is an important transcriptional factor for multiple proteins involved in the cellular damage response. Physiological p53 response prevents mutations from accumulating by increasing the expression of genes that inhibit cell growth, a predominant characteristic of cancerous cells (8). Frataxin was demonstrated to be a tumor suppressor protein (9, 10). Some connections between p53 and frataxin have been also established. For instance, the increase in lifespan by reduced expression frh-1, a frataxin homologue was significantly suppressed in the absence of cep-1, a p53 homologue. More directly, colon carcinoma cells, in which p53 is mutated or lost, lack expression of endogenous frataxin whereas human primary fibroblasts express this protein. Lately, we have shown the possibility that tumor-suppressor factor p53 controls the expression of mouse frataxin and the defects in tumor cells may cause the accumulation of ALA-induced protoporphyrin (7). Thus far, a question is raised that whether this model is conserved in human.

To clarify the decreased expression of frataxin in cancerous cells by the dysfunction of p53, we examined the p53-dependent regulation of frataxin in non-tumor cells. Here, we report that down-regulation of p53 decreased the level of human frataxin and identified the p53-responsive element in the promoter of the human frataxin gene. Improvement of the utilization of iron for heme biosynthesis by the expression of frataxin is also shown.

Materials and methods

Materials

Restriction endonucleases and DNA-modifying enzymes were from Takara Co. (Tokyo, Japan) and Toyobo Co. (Tokyo, Japan). Pifithrin-α was a product of Sigma-Aldrich (St. Louis, MI). Iron citrate was prepared as described previously (11). Antibodies for p53 and frataxin were as previously described (7). Polyclonal antibody for actin was obtained from Santa Cruz Biotechnology (Santa Cruz, CA). All other chemicals were of analytical grade.

Cell cultures and analysis of protoporphyrin

Human epithelial cervical cancer HeLa cells and human embryonic kidney HEK293T cells were grown in DMEM supplemented with 7% FCS and antibiotics. HeLa cells overexpressing frataxin (7) were incubated with 500 μM 5-aminolevulinic acid (ALA) for 4 h. After washing the cells twice with PBS, protoporphyrin in the cells was determined by fluorospectrophotometry (5, 12).

Reporter assay

The promoter region of the human frataxin gene was amplified by PCR using human genomic DNA. Reporter plasmids pGLFXN(-422), pGLFXN(-256), pGLFXN(-223), pGLFXN(-199), and pGLFXN(-178) were made as follows: PCR amplification was performed with antisense primer 5'-AAAAGCTTGCTGCTCCGGGTCTGCCGC-3' and the following sense primers: 5'-AAGAGCTCCACGAGGTCAGTAGATC-3' for pGLFXN(-422); 5'-AAGAGCTCTCGCACCACTGCCCTCCA-3' for pGLFXN(-256), 5'-AAGAGCTCGAATTTTATAAAACGCAT-3' for pGLFXN(-223); 5'-AAGAGCTCTGGTCACACAGCTAGGA-3' for pGLFXN(-199); and 5'-AAGAGCTCACAGAGAGGTTAATTAA-3' for pGLFXN(-178). Amplified fragments were subcloned into *Sac*I/*Hind*III-digested pGL4.10. The luciferase reporter plasmids containing minimal promoter, tk-luc-p53RE and tk-luc-p53REM, were constructed as follows: Double-stranded oligonucleotides containing frataxin p53RE (5'-AGCTTAACTTGCCCTCTGGTCACACAGCTAGGA-3') or p53RE(M) (5'-AGCTTAAaTTGCCCTCTGGTCACACAGCTAGGA-3') were phosphorylated and ligated into the Hind*III*-Bam*HI*-digested tk-luc (13).

For the expression of human p53 in HeLa cells, p53 cDNA was obtained by PCR from a human kidney cDNA library (Clontech Co., Mountain View, CA) using primers 5'-AATCTAGAACTGCCATGGAGGAGTCA-3' and 5'-AAAAGCTTCTAGCAGTTTGGGCTTTC-3'. The resulting amplicon was digested with *Xba*I and *Hind*III and inserted into *Xba*I/*Hind*III-digested pCG-N-HA (7). Cells were transfected with the reporter plasmids pGL4.10, pGLFXN (-422), pGLFXN (-256), pGLFXN (-223), pGLFXN (-199), pGLFX (-178), and pRL-RSV (Promega Co., Madison, WI) using lipofectamine 2000 (Life

Technologies, Carlsbad, CA), according to the manufacturer's recommendations. The cells were incubated overnight after the transfection and then washed twice with PBS. The cells were lyzed in Reporter lysis buffer (Promega Co., Madison, WI), the lysate was centrifuged, and the supernatants were assayed for luciferase. *Photinus* and *Renilla* luciferase assays were performed, according to the protocol for the Dual Luciferase Assay System (Promega Co.) (7, 13). Transfection efficiency was normalized on the basis of *Renilla* luciferase activity.

Chromatin immunoprecipitation

HEK293T and HeLa cells (1 x 10^8) were fixed in 20 ml of DMEM with 1% formaldehyde at room temperature for 10 min. Immunoprecipitations with monoclonal antibody for p53 were performed, followed by isolation of immunoprecipitates with protein G-Sepharose beads (Takara Co.). Real-time PCR reactions were carried out as described previously (7, 13). Primers 5'-TCACAGAGAGGTTAATTAA-3' and 5'-GCTGCTCCGGGTCTGCCGC-3' were used to amplify the DNA fragment of the p53 binding site.

2.5. Electrophoretic mobility shift assay (EMSA)

Nuclear extracts were prepared from HEK293T cells by the method of Schreiber *et al.*, (14). The biotin-labeled probe 5'-TTAACTTGCCCTCTGGTCACACAGCTAGGAA-3' was annealed with an equimolar amount of 5'-TTCCTAGCTGTGTGACCAGAGGGCAAGTTAA. EMSA was carried out, according to the protocol for the EMSA kit (Active Motif, Carlsbad, CA). The oligonucleotides containing mutated sites used in competition experiments were 5'-TTAAATTGCCCTCTGGTCACACAGCTAGGAA-3' and 5'-TTCCTAGCTGTGTGACCAGAGGGCAATTTAA-3' p53RE(M).

Immunoblotting

The lysates from HEK293T cells were subjected to SDS-PAGE and electroblotted onto PVDF membrane (Bio-Rad Laboratories, Hercules, CA). Immunoblotting was carried out, as described (7, 12).

Statistics

Results are shown as mean ± S.D. and were analyzed using unpaired Student's t-test. All statistical analyses were considered significant at the level of $p<0.05$ using GraphPad Prism software version 5.02 (GraphPad Software, Inc., CA) (7, 12).

Results

Expresson of frataxin is regulated by p53

To examine whether the expression of human frataxin is regulated by p53, non-tumor HEK293T cells were treated with an inhibitor of the p53 function, 5 μM pifithrin-α, for 16 h and the RT-PCR was carried out after the isolation of RNA. As shown in Fig. 1A, the level of frataxin mRNA in

pifithrin-α-treated cells was markedly decreased, compared with that in untreated cells. Immunoblot analysis revealed that frataxin in HEK293T cells was decreased by the treatment with pifithrin-α for 24 h (Fig. 1B). We next performed knockdown of p53 in HEK293T cells by siRNA and examined the expression of frataxin mRNA. A reduction of the expression of p53 mRNA resulted in the decrease of frataxin (Fig. 1C). Conversely, when wild-type p53 was expressed in tumor HeLa cells, the level of frataxin mRNA was higher than that of the control (Fig. 1D). These results indicated that the expression of human frataxin was p53-dependent.

p53-dependent control of the transcription of the human frataxin gene

Figure 2A shows the promoter sequence of the human frataxin gene. We found four sequences perfectly matched to the consensus sequence of p53-responsive element (p53RE) at -2,396 to-2,387 bp, -1,301 to -1,292 bp, and -328 to -319 bp located upstream of the putative start site of transcription, and at +109 to 118 bp in the intron 1 (INT1). We isolated the DNA fragments corresponding to p53RE located at -2396 to -2387, -1301 to -1292, and INT1 (+109 to 118), after which they were inserted into the tk-luc plasmid and examined for their transcriptional activities. However, no enhancement of activity was observed with the three plasmid constructs (data not shown). Then, we examined the transcriptional activity of the proximal region of the frataxin gene. Possible sequences corresponding to p53RE were found at -328 to -319 bp, -232 to -223 bp, -209 to -200 bp, and -189 to -180 bp in the proximal region of the promoter. To explore the function of these putative p53REs, we first examined the promoter activity. The 422-bp DNA fragment containing four p53REs was cloned into the pGL4.10 plasmid. The plasmids of differential deletion mutants were subsequently constructed. The expression of luciferase was analyzed by transfection of pGLFXN (-422), pGLFXN (-256), pGLFXN (-223), and pGLFXN (-199) into HEK293T cells. Compared with the activity of pGL-FXN (-178) without p53RE, pGL-FXN (-422), pGL-FXN (-256), and pGL-FXN (-223) showed high activity (Fig. 2B). The pGL-FXN-M (-199) containing one p53 RE showed the low activity. The reporter assay was also carried out with tumor HeLa cells expressing mutated p53 (Scheffner et al., 1991; Sawamoto et al., 2013). The activities with or without p53RE in HeLa cells were low and did not exhibit any response to p53. When HEK293T cells were treated with pifithrin-α, the activity of pGLFXN (-422) was markedly lowered, compared with that seen in control cells while that of pFXN(-178) was slightly decreased by the treatment (Fig. 2C). These results suggest that p53RE can me located at -209 to -200 bp in the promoter.

To verify that the p53RE (-209 to -200 bp) in the promoter is involved in p53-dependent regulation of the reporter gene, activities of a reporter plasmid, tk-luc, carrying p53RE or mutated p53RE were examined with HEK293T cells. As shown in Fig. 3A, the luciferase activity of tk-p53RE-M in HEK293T cells was less than that of the wild-type control tk-p53RE. When the wild-type p53 was expressed in HeLa cells, the activity of tk-p53RE, but not tk-luc, markedly

increased (Fig. 3B). Competitive assay of EMSA using biotin-labeled p53RE probe was carried out by the addition of an excess amount of mutated p53RE fragment. The specific band was diminished with an excess amount of the p53RE oligonuleotide (Fig. 4A). The mutation of a single nucleotide from T to A in the inside of p53RE diminished the competition. Furthermore, the treatment of nuclear extracts with antibody for p53 also diminished the formation of the DNA-protein complex, indicating that the sequence at -209 to -200 of the human frataxin-p53RE was critically important in the p53-dependent activation of gene expression. To confirm the recruitment of p53 to the promoter region of the frataxin gene in HEK293T cells, we carried out a ChIP assay using anti-p53 antibody. The presence of the promoter in the chromatin immunoprecipitate was analyzed by semi-quantitative PCR using specific primers spanning p53RE of the frataxin gene (Fig. 4B). The binding of p53 to the site was found in the cells while this binding was not observed with control IgG. In contrast, the ChIP assay using HeLa cells did not show the binding of p53 to p53RE. These results indicated that the promoter region at -209 to -200 in the human frataxin promoter acts as p53RE.

The expression of frataxin improved utilization of mitochondrial iron in HeLa cells.

Our previous study showed that HeLa cells stably overexpressing frataxin exhibited decreased ALA-induced accumulation of protoporphyrin (7). We here examined the effect of iron citrate on the ALA-induced accumulation of protoporphyrin in frataxin-expressing HeLa cells. The increased expression of frataxin in HeLa cells was confirmed by immunoblotting (Fig. 4A). To examine the effect of iron citrate on the ALA-induced accumulation of protoporphyrin in HeLa cells, the cells were treated with 500 μM ALA in the absence or presence of iron citrate for 5 h. The treatment of the frataxin transfectants with 25 and 50 μM iron citrate led to marked decreases of the amount of protoporphyrin by 70 and 80%, compared with that in cells without iron citrate, respectively (Fig. 4B). Meanwhile, the decline of the accumulation of protoporphyrin in iron citrate-treated mock-DNA transfectants was less than that in untreated cells. These results suggest that the elevated expression of frataxin led to improvement of the iron utilization for heme biosynthesis in mitochondria.

Discussion

The present study first gave a direct evidence that the expression of human frataxin is dependent on p53. Evidently, the inhibition of p53 function by pifithrin-α and the knockdown of p53 decreased the levels of frataxin mRNA and protein. The reporter activity of the promoter in the human frataxin gene carrying p53RE located at -209 to -200 bp was high in non-tumor HEK293T cells, but did not change in cancerous HeLa cells, compared with that without p53RE. The expression of frataxin as well was found to be stimulated in HeLa cells expressing mutated p53 (15) by expression of the wild-type p53. EMSA showed the binding of p53 to the frataxin p53RE, and the ChIP assay of the human frataxin promoter revealed that p53 was associated with p53RE in HEK293T cells, but not in

the case of HeLa cells. These findings supported the previous data that the expression of mouse frataxin was controlled by p53, and cells expressing wild-type p53 produced frataxin protein more than tumor cells with mutated p53 (7).

CHIP assay has revealed that the binding of p53 to the frataxin p53RE occurred in HEK293T cells, but not in HeLa cells (Fig. 4). High-grade tumor and malignant HeLa cells do not produce detectable p53 protein (15, 16). Based on the observation that in rat astrocytic tumors or tumor cell lines, a reduced level of was observed, as compared with its level in astrocytes (17), rat frataxin can be also regulated by p53 The present study showed that the transcription of the human frataxin gene was activated under the control of p53, and was low due to the mutation of p53 in Colo201, A431, and HeLa cells (7). It was also reported that human primary fibroblasts express a considerable level of frataxin, but colon carcinoma MIP101, DLD2 and HT29 cells do not produce frataxin protein (18). In addition, the active non-transformed cells highly expressed frataxin (18). Taking these findings, p53 positively regulates the utilization of mitochondrial iron for biogenesis of the iron-sulfur cluster proteins through the expression of frataxin.

We previously reported that the expression of frataxin in human tumor A431 cells was low and the FECH activity was increased by the expression of frataxin (12). FECH was interacted with frataxin, demonstrated by their co-expression in *E. coli* (7), yeast (19, 20) and human cells (21) and the iron chaperone frataxin's interaction with FECH may contribute to the maturation of FECH in mammalian mitochondria by biogenesis of the 2Fe-2S cluster at the carboxyl terminus. It has been noted that the overexpression of frataxin in human cancerous A431 cells increased the FECH activity, which decreased the ALA-induced accumulation of protoporphyrin (7). Conversely, the combination of the decrease of maturation of FECH with lowering of the iron supply by reduced expression of frataxin causes the ALA-induced accumulation of protoporphyrin and photosensitivity of tumor cells.

Aconitase consists of a 4Fe-4S cluster and its activity can be controlled by frataxin (22) since the enzyme activity in frataxin-overexpressing human colon carcinoma MIP101 cells is higher than that in mock DNA-transfected cells (10, 22). The level of the 2Fe-2S cluster-containing FECH in A431 cells also did not change by the overexpression of frataxin, while the enzyme activity in frataxin-overexpressing cells increased (7). Considering that the activities of both enzymes are dependent on the intracellular level of iron (22, 23), frataxin promotes the assembly of Fe-S clusters of respitory enzymes in mitochondria. This is supported by the finding that oxidative phosphorylation and ATP synthesis were enhanced by the expression of frataxin in tumor cells (10).

The mutation of p53 in cancerous cells gives rise to abnormal iron metabolism and dysfunction of mitochondria (24, 25). Given the fact that the expression of frataxin is induced under stress conditions and associated with p53 function (26), p53-defective cancer cells decrease the expression of mitochondrial enzymes involved in iron and heme metabolism. In contrast, the expression of frataxin

in human glioblastoma cells decreased the mitochondrial level of ROS, but increased the cytoplasmic level of ROS, due to the decrease of detoxification enzymes, resulting in high susceptibility to oxidant drugs (17). These discrepancies can be due to the different level of ectopic expression of frataxin in tumor cells or different types of tumor. The overexpression of frataxin protects tumor cells from apoptosis, but frataxin can also act as a tumor suppressor (9, 17, 27, 28). Therefore, regulation of the expression and function of frataxin in p53-mutated tumor cells is distinct from p53-induced regulation of frataxin in normal cells. Very recently, Shen et al.(29) found that heme directly down-regulates the expression of p53 in normal cells. Since frataxin is a target of p53, the utilization of iron and/or heme by a decrease of frataxin accumulates iron in mitochondria, produces excess ROS, and damages intracellular structures including proteins and DNA.

The expression of frataxin was found to be low in human cancerous cells (7, 17), and reduction of its function in cancerous cells leads to the decrease of mitochondrial function, including 2Fe-2S-containing FECH. The present data revealed that HeLa cells stably overexpressing frataxin accumulated less protoporphyrin from ALA than mock DNA-transfected cells. This is consistent to our previous study (7). However, also in the publication mentioned, the change of FECH was not obvious. Thus, the ALA-PDT outcomes may come from efficient ability of this chelating enzyme or possibly other impacts of frataxin on the apoptosis following therapy. The low accumulation of protoporphyrin in frataxin transfectants can be due to improvement of the mitochondrial function, including in terms of oxidative phosphorylation and iron utilization for heme biosynthesis. Frataxin may also deliver iron to other mitochondrial proteins including FECH, aconidase, and succinate dehydrogenase (21, 22, 30). These results are consistent with the observation that the overexpression of frataxin in cancerous cells decreased ROS production and induced mitochondrial functions, including respiratory function, membrane potential, and ATP production (10). Although the regulation of frataxin by p53 is affirmed in the present study, further ones will be required to clarify p53-frataxin-accumulation of protoporphyrin concept in order to complete the ALA-PDT.

References

1. Koeppen, A. H. (2011) Friedreich's ataxia: pathology, pathogenesis, and molecular genetics. *J Neurol Sci* **303**, 1-12.

2. Patel, P. I. and G. Isaya (2001) Friedreich ataxia: from GAA triplet-repeat expansion to frataxin deficiency. *Am J Hum Genet* **69**, 15-24.

3. Calabrese, V., R. Lodi, C. Tonon, V. D'Agata, M. Sapienza, G. Scapagnini, A. Mangiameli, G. Pennisi, A. M. Stella and D. A. Butterfield (2005) Oxidative stress, mitochondrial dysfunction and cellular stress response in Friedreich's ataxia. *J Neurol Sci* **233**, 145-62.

4. Thierbach, R., T. J. Schulz, F. Isken, A. Voigt, B. Mietzner, G. Drewes, J. C. von Kleist-Retzow, R. J.

Wiesner, M. A. Magnuson, H. Puccio, A. F. Pfeiffer, P. Steinberg and M. Ristow (2005) Targeted disruption of hepatic frataxin expression causes impaired mitochondrial function, decreased life span and tumor growth in mice. *Hum Mol Genet* **14**, 3857-64.

5. Ohgari, Y., Y. Nakayasu, S. Kitajima, M. Sawamoto, H. Mori, O. Shimokawa, H. Matsui and S. Taketani (2005) Mechanisms involved in delta-aminolevulinic acid (ALA)-induced photosensitivity of tumor cells: relation of ferrochelatase and uptake of ALA to the accumulation of protoporphyrin. *Biochem Pharmacol* **71**, 42-9.

6. Ye, H. and T. A. Rouault (2010) Human iron-sulfur cluster assembly, cellular iron homeostasis, and disease. *Biochemistry* **49**, 4945-56.

7. Sawamoto, M., T. Imai, M. Umeda, K. Fukuda, T. Kataoka and S. Taketani (2013) The p53-dependent expression of frataxin controls 5-aminolevulinic acid-induced accumulation of protoporphyrin IX and photo-damage in cancerous cells. *Photochem Photobiol* **89**, 163-72.

8. Liu, D. and Y. Xu (2011) p53, oxidative stress, and aging. *Antioxid Redox Signal* **15**, 1669-78.

9. Shoichet, S. A., A. T. Baumer, D. Stamenkovic, H. Sauer, A. F. Pfeiffer, C. R. Kahn, D. Muller-Wieland, C. Richter and M. Ristow (2002) Frataxin promotes antioxidant defense in a thiol-dependent manner resulting in diminished malignant transformation in vitro. *Hum Mol Genet* **11**, 815-21.

10. Schulz, T. J., R. Thierbach, A. Voigt, G. Drewes, B. Mietzner, P. Steinberg, A. F. Pfeiffer and M. Ristow (2006) Induction of oxidative metabolism by mitochondrial frataxin inhibits cancer growth: Otto Warburg revisited. *J Biol Chem* **281**, 977-81.

11. Taketani, S. and R. Tokunaga (1981) Rat liver ferrochelatase. Purification, properties, and stimulation by fatty acids. *J Biol Chem* **256**, 12748-53.

12. Ohgari, Y., Y. Miyata, T. Miyagi, S. Gotoh, T. Ohta, T. Kataoka, K. Furuyama and S. Taketani (2011) Roles of porphyrin and iron metabolisms in the delta-aminolevulinic acid (ALA)-induced accumulation of protoporphyrin and photodamage of tumor cells. *Photochem Photobiol* **87**, 1138-45.

13. Gotoh, S., T. Nakamura, T. Kataoka and S. Taketani (2011) Egr-1 regulates the transcriptional repression of mouse delta-aminolevulinic acid synthase 1 by heme. *Gene* **472**, 28-36.

14. Schreiber, E., P. Matthias, M. M. Muller and W. Schaffner (1989) Rapid detection of octamer binding proteins with 'mini-extracts', prepared from a small number of cells. *Nucleic Acids Res* **17**, 6419.

15. Scheffner, M., K. Munger, J. C. Byrne and P. M. Howley (1991) The state of the p53 and retinoblastoma genes in human cervical carcinoma cell lines. *Proc Natl Acad Sci U S A* **88**, 5523-7.

16. Nigro, J. M., S. J. Baker, A. C. Preisinger, J. M. Jessup, R. Hostetter, K. Cleary, S. H. Bigner, N. Davidson, S. Baylin, P. Devilee and et al. (1989) Mutations in the p53 gene occur in diverse human tumour types. *Nature* **342**, 705-8.

17. Kirches, E., N. Andrae, A. Hoefer, B. Kehler, K. Zarse, M. Leverkus, G. Keilhoff, P. Schonfeld, T. Schneider, A. Wilisch-Neumann and C. Mawrin (2011) Dual role of the mitochondrial protein frataxin in

astrocytic tumors. *Lab Invest* **91**, 1766-76.

18. Ristow, M., M. F. Pfister, A. J. Yee, M. Schubert, L. Michael, C. Y. Zhang, K. Ueki, M. D. Michael, 2nd, B. B. Lowell and C. R. Kahn (2000) Frataxin activates mitochondrial energy conversion and oxidative phosphorylation. *Proc Natl Acad Sci U S A* **97**, 12239-43.

19. Lesuisse, E., R. Santos, B. F. Matzanke, S. A. Knight, J. M. Camadro and A. Dancis (2003) Iron use for haeme synthesis is under control of the yeast frataxin homologue (Yfh1). *Hum Mol Genet* **12**, 879-89.

20. Park, S., O. Gakh, H. A. O'Neill, A. Mangravita, H. Nichol, G. C. Ferreira and G. Isaya (2003) Yeast frataxin sequentially chaperones and stores iron by coupling protein assembly with iron oxidation. *J Biol Chem* **278**, 31340-51.

21. Bencze, K. Z., T. Yoon, C. Millan-Pacheco, P. B. Bradley, N. Pastor, J. A. Cowan and T. L. Stemmler (2007) Human frataxin: iron and ferrochelatase binding surface. *Chem Commun (Camb)*, 1798-800.

22. Bulteau, A. L., H. A. O'Neill, M. C. Kennedy, M. Ikeda-Saito, G. Isaya and L. I. Szweda (2004) Frataxin acts as an iron chaperone protein to modulate mitochondrial aconitase activity. *Science* **305**, 242-5.

23. Taketani, S., Y. Adachi and Y. Nakahashi (2000) Regulation of the expression of human ferrochelatase by intracellular iron levels. *Eur J Biochem* **267**, 4685-92.

24. Zhou, S., S. Kachhap and K. K. Singh (2003) Mitochondrial impairment in p53-deficient human cancer cells. *Mutagenesis* **18**, 287-92.

25. Matoba, S., J. G. Kang, W. D. Patino, A. Wragg, M. Boehm, O. Gavrilova, P. J. Hurley, F. Bunz and P. M. Hwang (2006) p53 regulates mitochondrial respiration. *Science* **312**, 1650-3.

26. Asher, G., J. Lotem, B. Cohen, L. Sachs and Y. Shaul (2001) Regulation of p53 stability and p53-dependent apoptosis by NADH quinone oxidoreductase 1. *Proc Natl Acad Sci U S A* **98**, 1188-93.

27. Schoenfeld, R. A., E. Napoli, A. Wong, S. Zhan, L. Reutenauer, D. Morin, A. R. Buckpitt, F. Taroni, B. Lonnerdal, M. Ristow, H. Puccio and G. A. Cortopassi (2005) Frataxin deficiency alters heme pathway transcripts and decreases mitochondrial heme metabolites in mammalian cells. *Hum Mol Genet* **14**, 3787-99.

28. Guccini, I., D. Serio, I. Condo, A. Rufini, B. Tomassini, A. Mangiola, G. Maira, C. Anile, D. Fina, F. Pallone, M. P. Mongiardi, A. Levi, N. Ventura, R. Testi and F. Malisan (2011) Frataxin participates to the hypoxia-induced response in tumors. *Cell Death Dis* **2**, e123.

29. Shen, J., X. Sheng, Z. Chang, Q. Wu, S. Wang, Z. Xuan, D. Li, Y. Wu, Y. Shang, X. Kong, L. Yu, L. Li, K. Ruan, H. Hu, Y. Huang, L. Hui, D. Xie, F. Wang and R. Hu (2014) Iron Metabolism Regulates p53 Signaling through Direct Heme-p53 Interaction and Modulation of p53 Localization, Stability, and Function. *Cell Rep* **7**, 180-93.

30. Gonzalez-Cabo, P., R. P. Vazquez-Manrique, M. A. Garcia-Gimeno, P. Sanz and F. Palau (2005) Frataxin interacts functionally with mitochondrial electron transport chain proteins. *Hum Mol Genet* **14**, 2091-8.

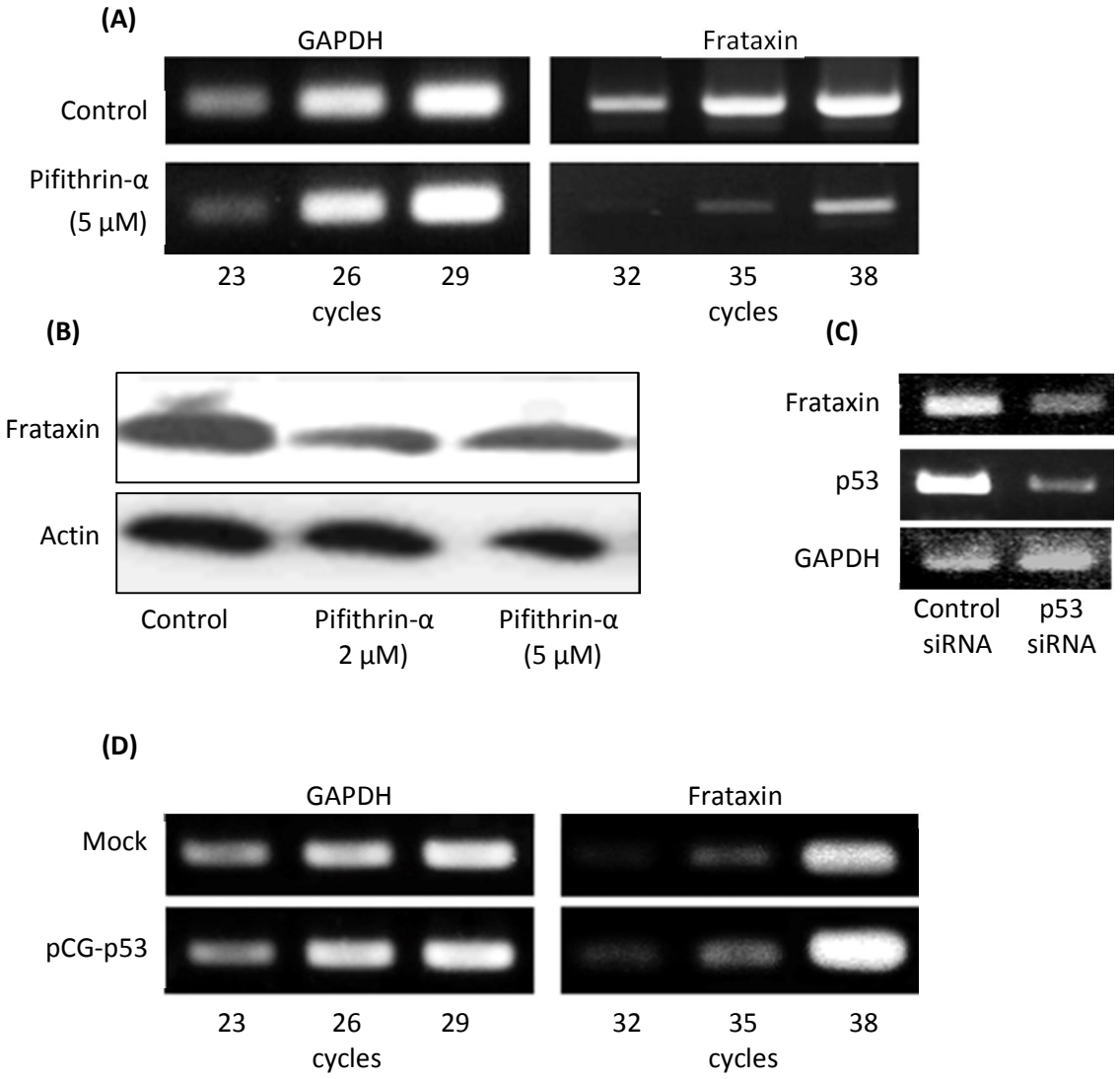

Figure 1. The regulation of the expression of frataxin by p53. (A) The decrease of the expression of frataxin mRNA by the inhibition of the p53 function. RNA was isolated from HEK cells treated with Pifithrin-a for 16h. After single stranded cDNA was synthesized, the indicated cDNA fragment was amplified by PCR. (B) Immunoblot analysis. The cells were treated as above. Proteins of the cells were analyzed by SDS-PAGE and electroblotted onto PVDF membrane. Immunoblotting was performed using anti-frataxin and anti-actin antibodies as the primary antibody. (C) Knockdown of p53. HEK cells were transfected with control RNA or p53siRNA and cultured for 48h. RT-PCR was carried out with primers of p53 and frataxin. (D) Increase in the expression of frataxin by p53. HeLa cells transfected with mock DNA or pCG-HA-p53 were cultured for 16h. RT-PCR was carried out using the indicated promers.

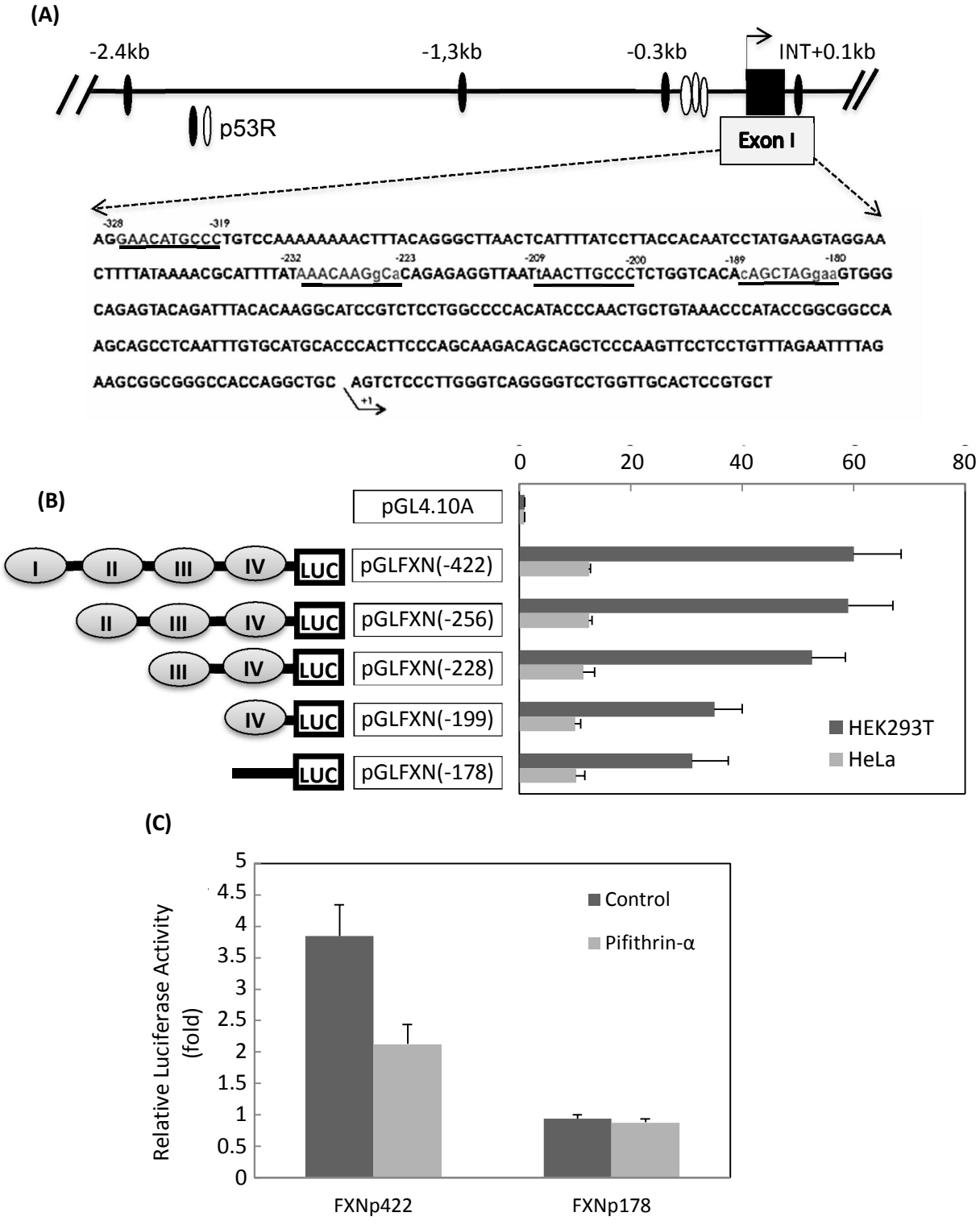

Figure 2. Functional assay of the p53-dependent transcription of the human frataxin gene. (A) The nucleotide sequence of the promoter region of human frataxin gene. The putative p53 REs are underlined. The p53RE in the upstream region shows variant nucleotides compared with the consensus decamer: PuPuPuC(A/T)(A/T)GPyPyPy. The transcription start site is shown as +1. (B) The reporter activity of the human frataxin gene. HEK293T cells and HeLa cells were transfected

with pGL4.10 (Promega Co.), pGLFXN (422), pGLFXN (256), pGLFXN (223), pGLFXN (199), pGLFXN (178) and pRL-RSV vectors, and cultured for 16 h. Luciferase activity was measured and normalized to the *Renilla* luciferase activity. Data are the average of 3 independent experiments (Bars=S.D.). (C) Effect of the expression of wild type p53 on the transcriptional activity in HeLa cells. The cells were transfected with a luciferase reporter plasmid pGLFXN (422) containing the frataxin promoter or p53RE-deleted pGLFXN (178), pCG-HA-p53 or empty vector (pCG) and cultured for 16 h. The reporter activity was measured.

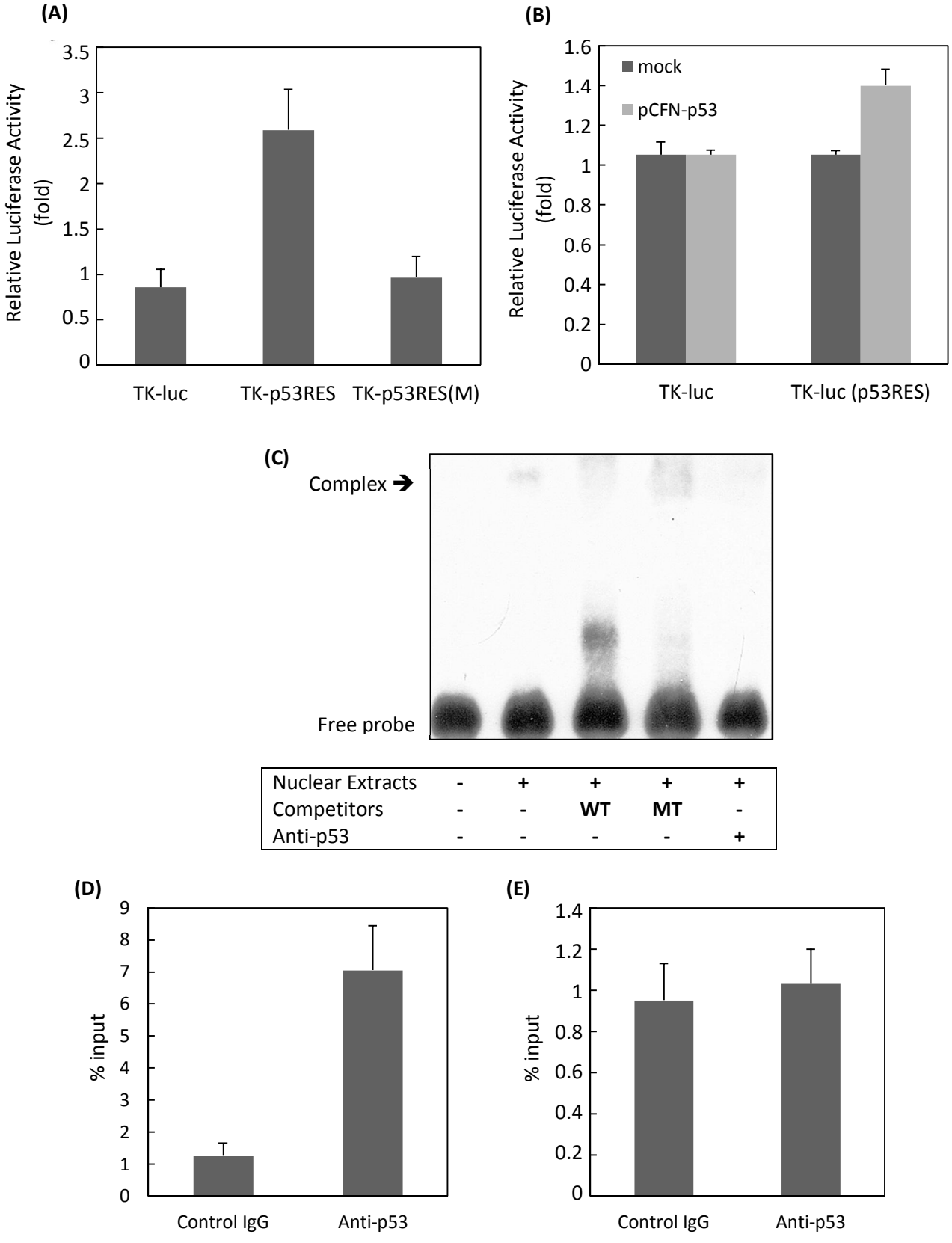

Figure 3. p53-dependent transcription activity of the human frataxin gene. (A) Identification of the human p53RE. HEK cells were transfected with a luciferase reporter plasmid containing the human p53RE or one containing mutated p53RE. Luciferase activity was measured and normalized to *Renilla*

luciferase activity. The data are the average ±SD of at least three independent experiments (* P <0.01, mutated p53RE versus p53RE). (B) Effect of wild type p53 expression. HeLa cells were transfected with a luciferase reporter plasmid containing the human p53RE or one containing mutated p53RE, pCG-HA-p53 or empty vector (pCG) and cultured for 16 h. The reporter activity was measured.

The binding of p53 to the human frataxin p53RE. (C) EMSA of the frataxin-p53RE oligonucleotide-binding activity in HEK cells. EMSA using biotin-labeled frataxin-p53RE was performed with nuclear extracts from the cells. A 50-fold excess amount of unlabeled frataxin-p53RE (WT) or mutated frataxin-p53RE (MT) oligonucleotides were used, as competitors. EMSA was carried out using the reaction mixture incubated with biotin-labeled frataxin-p53RE at room temperature for 10 min. The preincubation of nuclear extracts with antibodies for p53 was carried out at 4ºC for 10 min. After the DNA-protein complexes were separated using 4% polyacrylamide gel, they were blotted onto a nylon membrane. Biotin-oligonucleotides reacted with horseradish peroxidase-conjugated streptavidin, followed by detection with chemilumirescence. Arrows show the positions of the DNA-p53 complex. Binding of p53 to p53RE region of the human frataxin gene. A ChIP assay of p53 was performed with lysates from HEK (D) or HeLa (E) cells. The immunoprecipitation reaction with mouse mormal IgG and anti-p53 antibody was carried out. Real-time PCR was performed to amplify the promoter region containing p53RE of the frataxin gene. Data are represented as fold enrichment compared with IgG control (* P <0.01).

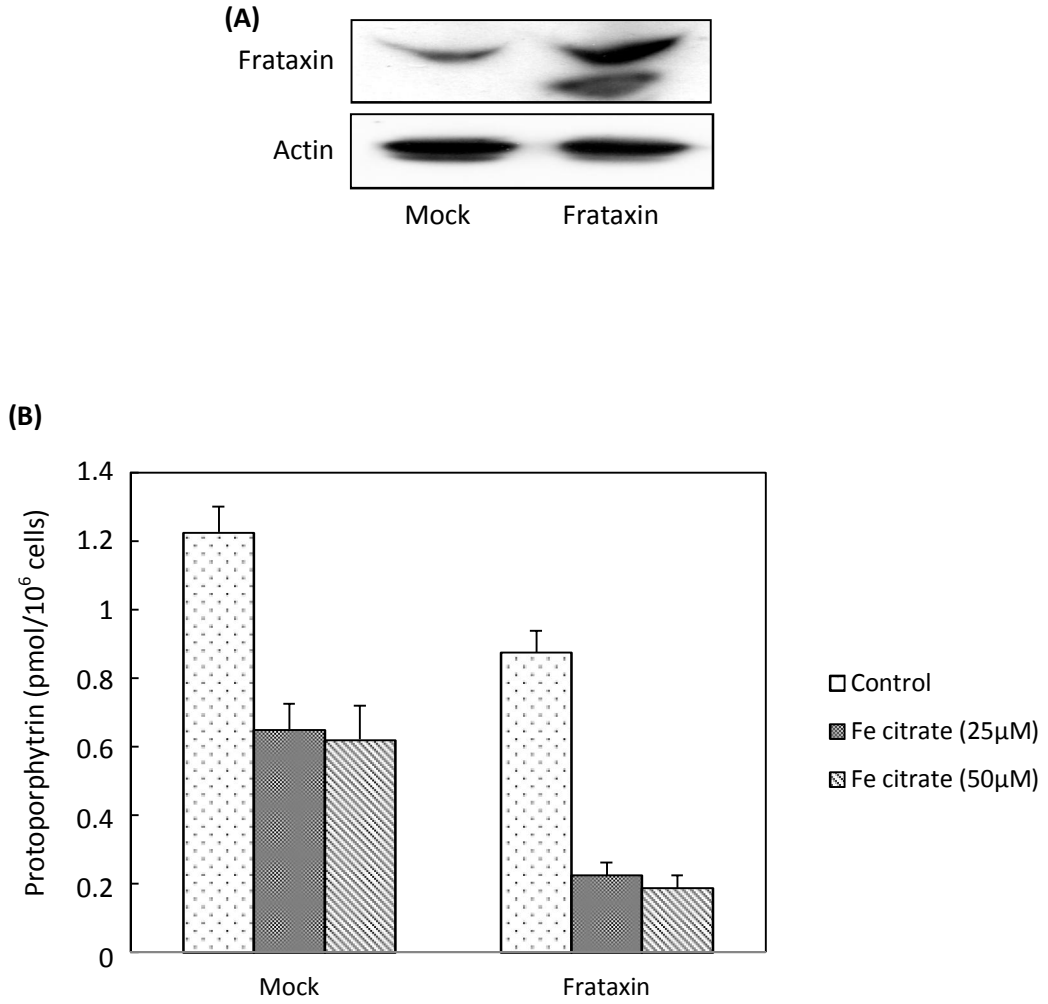

Figure 4. The ALA-induced accumulation of protoporphyrin in HeLa cells expressing frataxin. (A) Immunoblots. The lysates of the frataxin transfectants and mock-DNA transfected cells was separated by SDS-PAGE and then immunoblotting for frataxin and actin was performed. (B) The frataxin transfectants and mock-DNA transfected cells were incubated with 500 μM ALA for 16 h in the absence or the presence of the indicated concentration of iron citrate. The accumulation of protoporphyrin in frataxin transfectants and control cells incubated with 500 μM ALA plus 25 or 50 mM iron citrate for 16 h was estimated by fluorescence spectrophotometry. Data are expressed as the mean ± S.D. of triplicate experiments.

Conclusion

The lives of the cells and of the body as a whole are crucially dependent upon the biosynthesis and metabolism of porphyrins. Almost all types of cells of the human body, with the exception of mature red blood cells, are equipped with a machinery to synthesize heme. Although nearly all human cell types express the enzymes involved in the heme synthesis, a distinct activity of the enzymes in tumor as compared with normal cells leads to a higher PPIX accumulation within transformed cells. These facilitate the ALA-PDT. However, this therapy has its limitations. Despite the general tolerance, some patients have complained of stinging, burning, pricking, smarting and itching pain during PDT and several hours after irradiation.

At first, the present study apparently clarifies the penetration of ALA via two typical NTTs, SLC6A6 and SLC6A13, into tumor cells as well as their significant contribution to PDT. This elucidation should directly help to optimize this photo-based therapy by mediating the formation of photosensitizer through these transporters. Consequently, we could gain a better either control or modification of the diagnostic and treating applications. Besides, thanks to the primary sensory-nerve-ending location of these transporters, clarification of ALA uptake through NTTs initially provides a molecular explanation for clinical pain drawback of ALA as well as ALA-methylester-PDT, to which many patients have to face during the therapy. This finding as well might help to overcome the sufferings by impact on appropriate mechanisms.

In another approach, this study identified the p53-responsive element in the proximal promoter region of the human frataxin gene. In addition, the treatment of frataxin-overexpressing HeLa cells with iron citrate markedly decreased the ALA-induced accumulation of protoporphyrin. Not only the inhibition of p53 function but also the knockdown of p53 reduced frataxin, mRNA and increased the photosensitizer accumulation, addressing that the utilization of mitochondrial iron, which is relating to PPIX, is regulated by p53 via level of frataxin. Besides, from distinct regulation of the expression and function of frataxin between p53-mutated tumor cells and usual p53-induced regulation of frataxin in normal cells, FECH, the enzyme supposedly differentiates the outcomes of PDT between normal and tumor cells, is suggested to be regulated by the p53-frataxin complex. In brief, ALA-PDT possibly mediated through FECH by affecting on the p53-frataxin modality.

Thus far, in the relative comparison, management of effectiveness of ALA-PDT through import gateway, such as SLC6A6 and SLC6A13, is more facilitating than the p53-frataxin modality. This is due to the comprehensibly enzymatic conversion of the precursor ALA than handle multifunctional p53 and frataxin, which participate in many intracellular metabolisms with as yet unclarified mechanisms.

List of publications

1. Neurotransmitter transporter family including SLC6A6 and SLC6A13 contributes to the 5-aminolevulinic acid (ALA)-induced accumulation of protoporphyrin IX and photo-damage, through uptake of ALA by cancerous cells

   Photochemistry and Photobiology. (2014) In press.

2. p53 directly regulates the transcription of the human frataxin gene and its lack of regulation in tumor cells decreases the utilization of mitochondrial iron

   Gene. (2014) In press.

3. Imaging of heme/hemeproteins in nucleus of the living cells expressing heme-binding nuclear receptors

   FEBS (Federation of European Biochemical Societies) Letters 587 (2013), 2131-2136.

Acknowledgments

At first, I would like to express my sincerely deepest thanks to my supervisor, Professor SHIGERU TAKETANI. This thesis only could be finished with his kindly orientation, support and encouragement throughout the process.

I am grateful to Professor KAMEI KAEKO for her kind introduction, Professor PHAM DINH LUU, Associate Professor PHAM NGUYEN VINH, Associate Professor PHAM DANG DIEU and Vice Dean NGUYEN THE DUNG for giving me the chance to study in Kyoto Institute of Technology.

I also wish to thank co-worker, Associate Professor YASUSHI ADACHI from Department of Pathology, Toyooka Hospital, Toyooka, Hyogo and either past or present members of my laboratory, Professor IKUKO SAGAMI, Doctor KAZUSHIGE HAMADA, MD DAO HOANG THIEN KIM, MD NGUYEN NGOC LAN, ANFENG MU, YUSUKE HORI, ASAKO KAWAZOE, YUKA ADACHI, RINA SHIMIZU, RYUHEI ITOH and KEN-ICHI FUJITA for their valuable experiences and enthusiastic supports to help to accomplish this thesis.

I also acknowledge the scholarship from fund of Kyoto Institute of Technology, grants from Ministry of Health, Labor and Welfare and Ministry of Education, Science, Sports, and Culture of JAPAN.

And lastly, I would like to send my hearty thanks to my family. Thank all of you for always being beside, encouraging and sharing with me during the whole time of study.